UNIVERSIDADE
BEIRA INTERIOR

Conceptual Design of a Micro Two-Spool Turboprop Engine

Design Point and Parametric Study

Versão revista após defesa

Sisenando Machado Fontes

Dissertação para obtenção do Grau de Mestre em
Engenharia Aeronáutica
(mestrado integrado)

Orientador: Prof. Doutor Francisco Miguel Ribeiro Proença Brójo

Julho de 2020

Dedication

To my family, girlfriend and friends

Acknowledgements

I would like to express my sincere gratitude to Prof. Francisco Miguel Ribeiro Proença Brójo for all the guidance, availability and wisdom in carrying out this thesis.

I would also like to thank all the teachers who contributed to my academic formation.

I would like to thank all the friendships that I have made in Covilhã over the years, especially to all my friends of Aeronautical Engineering Course, Forum Veteranum, Tuna Orquestra Académica Já b'UBI & Tokuskopus and PES.

I would also like to thank one of my families, the Humanitarian Association of Famalicenses Volunteer Firefighters, for all the training, knowledge transmitted and for all the friendships that I made, mainly "Aço dos Guitas".

I want to express my thanks to Nélson Costa and Sofia Martins for all their friendship, love, patience, euphoria and for all the good times we spent together.

I also thank the Esteves Family for all the kindness and compassion they have always had with me.

I want to sincerely thank all my family, especially my parents, Sisenando and Maria Augusta, my brother Eduardo and my grandparents for all the love, care, for always believing in me and never giving up.

Finally, I would like to, especially, thank a lifetime love, my girlfriend, for all the love, dedication, patience and understanding she has had with me over the years.

Thank you all!

Resumo

Nesta tese foram realizados um ponto de projeto e um estudo paramétrico de um micro motor turboélice de dois veios.

O cálculo para o ponto de projeto é baseado nas equações de desempenho de um motor turboélice de dois veios que, posteriormente, será usado para obter o estudo em função da altitude, caudal de ar admitido, razão de pressões total do compressor, temperatura de entrada na turbina e velocidade de voo. O ponto de projeto é definido assumindo algumas variáveis devido à falta de informações disponíveis para um motor.

Posteriormente, é realizada uma análise paramétrica para entender o comportamento da ESFC, TSFC, PSFC, EPW e Fnet, variando a altitude, o caudal de ar, a razão de pressões do compressor, a temperatura de entrada da turbina e a velocidade de voo.

Palavras-chave

Turboélice, dois veios, ponto de projeto, estudo paramétrico, ESFC, TSFC, PSFC, EPW, Tração

Abstract

In this thesis, a design point of a micro two-spool turboprop engine is made as well as its parametric study. The calculation for a design point is based on performance equations for a two-spool turboprop engine which will later be used to obtain the study as a function of the altitude, air mass flow and turbine inlet temperature compressor total pressure ratio and flight speed.

The design point is made by assuming some variables due to the lack of information available for an engine. Afterwards, a parametric analysis is made to understand the behavior of ESFC, TSFC, PSFC, EPW and Fnet varying the altitude, airflow, pressure ratio, turbine inlet temperature and flight speed.

Keywords

Turboprop, two-spool, design point, parametric study, ESFC, TSFC, PSFC, EPW, Thrust

Contents

List of Figures

List of Tables

Nomenclature

Acronyms

CTPR	Compressor Total Pressure Ratio
HPT	High-pressure turbine
LPT	Low-pressure turbine
NGV	Nozzle guide vanes
TIT	Turbine Inlet Temperature
UAV	Unmanned Air Vehicles

Greek Symbols

ΔPb	Total pressure loss in combustor [kPa]
ΔPin	Intake pressure loss [dimensionless]
$\Delta Pj,pipe$	Total pressure loss of low-pressure turbine jet pipe [dimensionless]
$\Delta Pt,duct$	Total pressure loss in the duct between high- and low-pressure turbines [kPa/kPa]
β1	Compressor middle stage bleed air ratio [dimensionless]
γ	Specific heat ratio [dimensionless]
ε1	Compressor middle stage air extraction ratio for low-pressure turbine duct cooling [dimensionless]
ε2a	Cooling air ratio for high-pressure turbine[dimensionless]
ε2b	Cooling air ratio for low-pressure turbine duct[dimensionless]
ε3	Cooling air ratio NVG [dimensionless]
$\eta 2$	Compressor isentropic efficiency [dimensionless]
$\eta 416$	HPT isentropic efficiency [dimensionless]
$\eta 46$	LPT isentropic efficiency [dimensionless]
ηb	Combustor efficiency [dimensionless]
$\eta c,pol$	Compressor polytrophic efficiency [dimensionless]
ηm	Mechanical efficiency [dimensionless]
ηp	Propeller efficiency [dimensionless]
$\eta prop,d$	Propeller dynamic efficiency [dimensionless]
$\eta prop,s$	Propeller static efficiency [dimensionless]

ηt,pol	Turbine polytrophic efficiency [dimensionless]
Πc	Compressor total pressure ratio [dimensionless]
Πn	Exhaust nozzle pressure ratio [dimensionless]
Πt	Turbine total pressure ratio [dimensionless]

Roman Symbols

a_i	Speed of sound at engine station “i” [m/s]
A7	Exhaust nozzle area [m^2]
A7,c	Nozzle exit area for choking condition [m^2]
Cf	Thrust coefficient of Propeller [dimensionless]
Cpc	Specific heat for compressor [kJ/kgK]
Cpt	Specific heat for turbine [kJ/kgK]
Cpw	Power coefficient of Propeller [dimensionless]
d	Propeller diameter [m]
EPW	Equivalent shaft power [kW]
ESFC	Equivalent power specific fuel consumption [kg/(kW*h)]
f	Fuel air ratio [kg/kg]
Fnet	Net total thrust [N]
Fa	Nozzle thrust [N]
Gc	Power required for compressor [kW]
Ghpt	Power generated by high-pressure turbine [kW]
Glpt	Power generated by low-pressure turbine [kW]
J	Advance ratio [dimensionless]
Mo	Flight Mach number [dimensionless]
$\dot{m}$	Engine airflow at station “i” [kg/s]
$\dot{m}f$	Fuel flow [kg/s]
n	Propeller speed [rpm]
Ncd	Nozzle discharge coefficient [dimensionless]
Ncx	Nozzle thrust coefficient [dimensionless]
Pi	Total pressure in engine station "i" [kPa]
Pamb	Ambient static pressure [kPa]
PSFC	Power Specific fuel consumption [kg/(kW*h)]

PW	Uninstalled engine shaft power [kW]
Tamb	Ambient static pressure [K]
Tbleed	Compressor middle stage total temperature for bleed [K]
Ti	Total temperature at the station “i” [K]
TSFC	Thrust specific fuel consumption [kg/(kN)*s]
Vo	Aircraft flight speed [m/s]

Chapter 1

1. Introduction

Nowadays, there has been an increase in application of Unmanned Air Vehicles (UAV's) as well as the research to raise their performance (Large & Pesyridis, 2019). The UAV's can be used for various purposes, such as surveillance and small cargo transport. Depending on the purpose of the UAV, an electric engine may not be the most suitable, so micro gas turbine engines have been introduced and developed according to the mission's objective.

1.1 Motivation and Objectives

Micro gas turbines can have a very high number of design points that respect the flight requirements. Nevertheless, it is required much investigation to provide the engine with the best quality regarding the type of the UAV's mission. The present research is mainly focused on micro turboprop engines, nevertheless, not much information is available, being the principal source turbojet engines "due to the relative simplicity of manufacture" (Large & Pesyridis, 2019). The turboprop engine is very efficient at lower altitudes and lower velocities and the most suitable for medium-range missions. Since there is not much information about micro turboprop engines, in this work, the design point of a micro two-spool turboprop engine is made along with its parametric study. As the optimization of an engine is a lengthy process, this work also aims to be useful in future research work regarding the conceptual design of a micro two-spool turboprop engine.

1.2 Thesis Overview

This thesis is structured into five chapters, as follows:

Chapter 2 presents a literature review of gas turbines. It includes how a gas turbine works in a thermodynamic point of view and gives an overview of the main components of a turboprop engine.

Chapter 3 explains how to achieve the design point of the micro turboprop engine as well as the design input data used.

The parametric study is presented in chapter 4. It is also presented the discussion of the results given in the previous chapter.

Chapter 5 gives a conclusion of a design point and the parametric study of a micro two-spool turboprop engine and, also, some possible future works.

Chapter 2

2. Background

2.1 Gas Turbines

A gas turbine is an engine that uses the combustion of fuel in air to produce mechanical work. Is composed of three primary components mounted on the same shaft: the compressor, the combustion chamber and the turbine. Air enters the compressor where it is compressed by work transfer from the turbine. In the combustion chamber, the air is combined with fuel and burned, generating an increase of both temperature and specific volume. The combustion gases are fed into the turbine where they expand, which creates a positive shaft work transfer and then are exhausted to the atmosphere. If a gas turbine is modelled as an open system with air as the working fluid, this cycle is well-known as the Brayton cycle (El-Sayed, 2017). Thermodynamically speaking, the elementary operation of a gas turbine is a Brayton cycle.

2.1.1 Brayton Cycle

The Brayton cycle exemplifies the operation of a gas turbine engine (see figure 2.1). The first versions of this type of engines were vapor engines where air and fuel were mixed as they entered the compressor through a heated surface carburetor. The air/fuel mixture was contained in a tank, and then as the mixture entered an expansion cylinder, the fuel/air mixture is ignited by a pilot flame. A protection screen was used to prevent the fire

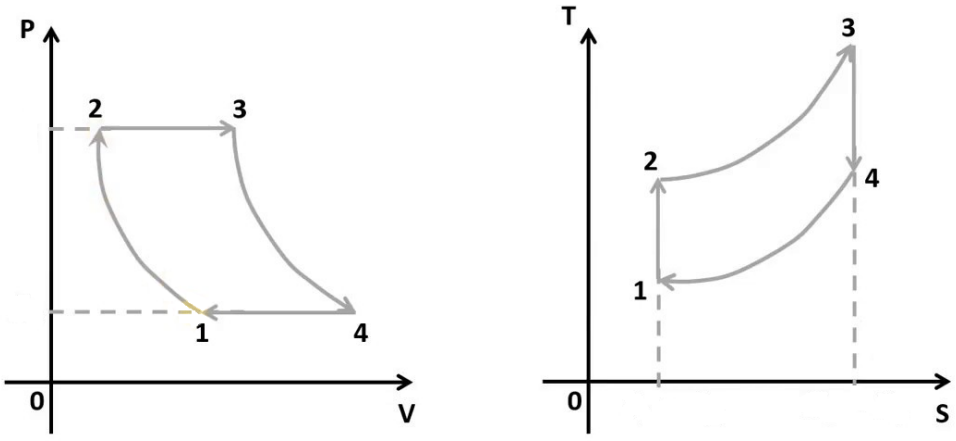

Figure 2.1 - Ideal Brayton cycle

to return to the tank. However, on the first attempts, the protection screens failed, and an explosion occurred. In the following years, many variations were made, mainly at a design level.

Although the first Brayton gas turbines were only made using a piston compressor and a piston expander, the modern Brayton engines use a compressor and a turbine for the compression and expansion processes, which have some differences when it comes to a thermodynamic level. The ideal Brayton cycle is composed of two isentropic and two isobaric processes.

Figure 2.2 presents the P-V and T-S diagrams for the ideal Brayton cycle. The process between stage 1 and stage 2s is the ideal intake and compression and represent the first isentropic process (1-2 is the real intake and compression process, which is only adiabatic), where the air is drawn into, slowed down and pressurized. The process between stages 2 and 3 represent the combustion and is the first isobaric process. In this section the fuel is burned, heat is added, entropy and volume increase and the temperature ranges to its maximum value. Since the combustion chamber is an open device, the pressure is constant in the process. The process between the stages 3 and 4s is the ideal expansion, and it is the second isentropic process (3-4 is the real expansion process, which is only adiabatic) where pressurized and heated air release his energy as it is expanded through a turbine and propelling nozzle. The pressure and the temperature decrease as the volume increases while the air flows through the turbine. In this stage, the heat is converted to mechanical work. Some of the turbine work is harnessed to drive the compressor. The process between stages 4 and 1 is the second isobaric process and represents the cooling of the gases to the initial temperature. In real gas turbines, the system is open to the environment, and this process does not exist, being part of the energy of the combustion eliminated with the exhaust gases.

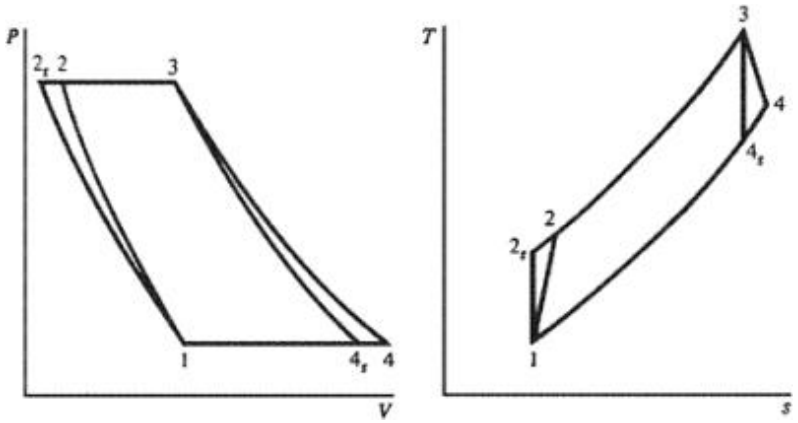

Figure 2.2 - Brayton cycle with ideal and adiabatic compression and expansion.

There are some variants of the Brayton cycle, such as the closed Brayton cycle, the solar Brayton cycle and the reverse Brayton cycle. In the closed Brayton cycle, the air expelled from the turbine is reintroduced in the compressor, and it is used a heat exchanger to heat the working fluid instead of a combustion chamber (Sinha & Narayan, 2015). It is differentiated by the fact that the working fluid is always in the vapor phase. The operation of this cycle generally occurs through the air inlet the compressor at a specific temperature and pressure. The cycle will have a maximum supported temperature and exhaust pressure at the compressor outlet. The compressor, turbine and overall cycle efficiency are calculated after gas circulation within the cycle. For better work and performance, it is often assumed that the air behaves as a perfect gas and has a constant specific heat value and that each process takes place permanently and there are no variations in kinetic or potential energy.

In the solar Brayton cycle, centered powerplants with hundreds or thousands of reflectors are positioned around a central tower. Each reflector tracks the sun to reflect radiation to the central receiver. Concentrated heat absorbed at the receptor is transferred to a circulating fluid that can be stored and/or used to produce work. The air allows the operation of a gas turbine, which enables the creation of a concentration tower electric generation plant, where the tower heats open-cycle air, may or may not have an additional burner, which vaporizes water in a heat exchanger for the operation of a steam turbine.

The Brayton cycle that drives in reverse is also known as a gas refrigeration cycle or Bell Coleman cycle. Its goal is to move heat from lower temperatures to higher temperatures, instead of producing work. This air-cooling technic is usually used in jet aircraft and for air-conditioning systems using bleed air tapped from engine compressors.

2.1.2 First Law analysis of Brayton cycle

The first law of thermodynamics is a form of the law of conservation of energy, and it states that energy can be converted from one form to another with the interaction of heat, work and internal energy, but can be neither created nor destroyed, under any circumstances.

Mathematically, the first law of thermodynamics for an open system, which in this case is a gas turbine, is

$$\frac{dU}{dT} = \dot{Q} - \dot{W}shaft + \sum_{in} \dot{m}\left(h + \frac{v^2}{2} + gz\right) - \sum_{out} \dot{m}\left(h + \frac{v^2}{2} + gz\right) \quad (2.1)$$

The first part of the equation represents the variation of the internal energy over time and on the second part, the first term represents the heat transferred in and out per unit of time, the second term represents the shaft work transferred per unit of time. The third and fourth term represents the energy that is convected out of the control volume by the mass flowing across the control surface per unit of time, where h represents the enthalpy, the term with velocity represents the kinetic energy of the term with z represents the potential energy (Tsai, 2004). The system inside the control volume is constant, so the energy variation inside the control volume is zero for steady flow processes. As the kinetic and potential energy variations are not significant factors for this analysis, they can be neglected, and the first law for steady flow processes becomes:

$$0 = \dot{Q} - \dot{W}shaft + \dot{m}(hin - hout) \quad (2.2)$$

Adiabatic compression is the first process of the Brayton cycle, which means that there is no heat transfer and the power required to run the compressor is

$$\dot{W}_{1-2} = \dot{m}(h1 - h2) \quad (2.3)$$

In the second process is an addition of heat at constant pressure and there is no shaft work transfer, so the heat per unit of time transferred is

$$\dot{Q}_{2-3} = \dot{m}(h3 - h2) \quad (2.4)$$

The third process is the second adiabatic process, where the heated working fluid is expanded through a turbine. There is no heat transfer, so the power transfer is

$$\dot{W}_{3-4} = \dot{m}(h3 - h4) \quad (2.5)$$

In the final process, the heat is rejected. As in the second process, there is no shaft work transfer, so the heat transfer per unit of time is

$$\dot{Q}_{4-1} = \dot{m}(h1 - h4) \quad (2.6)$$

2.2 Turboprop Engines

The turboprop engines are a variation of turbojet engines. They drive a propeller using the exhaust gases to drive the power turbine that is connected to a reduction gear by a shaft. The propeller performance is reached at a much slower speed than the turbine operation velocity. To use the propeller at peak performance, the propeller is coupled to the turbine through a reduction gear that converts high velocity, low torque output to low velocity, high torque. Comparing to a piston engine where the power output is measured in horsepower and is determined mainly by velocity and manifold pressure, the power of a turboprop is measured in shaft horsepower (shp), which is determined by velocity and the torque applied to the propeller shaft (FAA, 2016). However, some thrust is always produced by exhaust leaving the engine, since the turboprop engine is a gas turbine engine (usually less than 10% of the total engine power).

Since the propeller can move a large mass of air as the aircraft travels at a low ground and flight speed, it gives excellent performance during the takeoff and climbs to the turboprop engine, so on a standard day, the propeller of a turboprop engine is approximately 90% of total thrust at sea level conditions.

There are two primary varieties of turboprop engines:

- Single shaft/Fixed shaft engine.
- Free turbine/Split shaft engine.

Moreover, the main difference between them is how they drive the Propeller.

In the single-shaft engine presented in Figure 2.3, the air enters the compressor section through the engine inlet. While crossing the compressor, the air pressure increases, and the air is directed to the rear of the combustion chamber. In the combustion chamber, the fuel is added to the air where an igniter plug (only to start the engine) ignites the mixture. The combustion generates a high-speed expansion of the gases flow through the turbine where that energy will be converted into torque. The same shaft, where the compressor and turbine are connected, is connected to a reduction gear to convert high velocity/low torque to low velocity/high torque to drive the propeller. The exhaust air is expelled to the atmosphere by the propeller nozzle. Over 50% of the engine power is used to drive the compressor, about 20% of the compressed air is used to cool the system, pneumatic systems, cabin pressurization or heating and about 10% is used in the combustion process (FAA, 2016).

In this type of engine, the power changes are made by increasing the propeller blade angle and the fuel flow instead of engine speed. The increase in fuel flow means an increase in temperature and a corresponding increase in energy available to the turbine, which will be transmitted to the propeller in the form of torque—these increases in torque force the increase in blade angle to maintain the constant speed. The increase of the fuel flow is an essential factor to consider once this increase takes to an increase in temperature in the combustion chamber and turbine and must be limited to the strength and durability of these components' materials.

In short, in a single shaft engine, the same shaft drives the compressor and the Propeller (see example in Figure 2.3). The reduction gearbox reduces the engine shaft rotational speed once the propeller needs to rotate at a slower speed compared to a turbine speed and to accommodate the propeller through the propeller drive shaft.

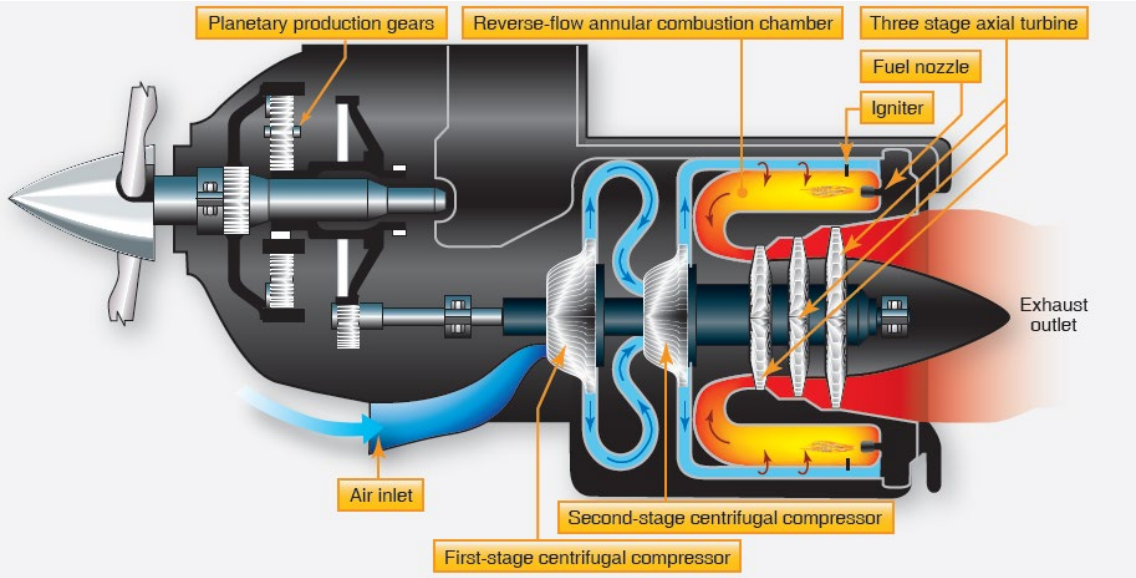

Figure 2.3 - Example of a fixed shaft turboprop engine (FAA,2016)

In a free turbine engine (see Figure 2.4) there are two shafts, one where a turbine drives the compressor, operating as a single unit as they run at a constant velocity independently of propellers speed, and one where a dedicated turbine drives the propeller. Since the propeller needs to rotate at lower velocities than the turbine, a reduction gearbox reduces the velocity to an adequate value.

There are many configurations for a free turbine engine. In figure 2.4, it is exemplified the Pratt & Whitney PT-6 engine. In this configuration, the air enters at the back of the engine, and unlike most of the engines, it flows forward through an axial flow compressor and a centrifugal flow compressor facing an increase in pressure and a change in direction

entering the combustion chamber. After the combustion, the gases direction is reversed again (forward) and they are expanded through the turbines. Finally, they are expelled to the atmosphere through the exhaust in the front of the engine.

The free turbine and reduction gearbox are assembled in the same shaft that drives the propeller. The compressor is assembled on the same shaft as the accessory gearbox. This accessory gearbox is used to provide power to drive fuel pumps and control, oil pumps, a tachometer transmitter and a starter/generator.

Another difference in this type of engine is in the powerplant operation, which is realized by three sets of controls:

- The power lever.
- The propeller lever.
- The condition lever.

The power lever controls the engine power in the range from idle through takeoff power. The motion forward or backward increases or decreases, respectively, gas generator velocity and consequently, increases or decreases engine power. The propeller lever controls the constant speed of the Propeller through the primary governor. The Propeller usually rotates from 1500 to 1900 rpm. The condition lever controls the fuel flow to the engine, and it is just an on/off valve for delivering fuel. This task is performed automatically by a devoted fuel control unit.

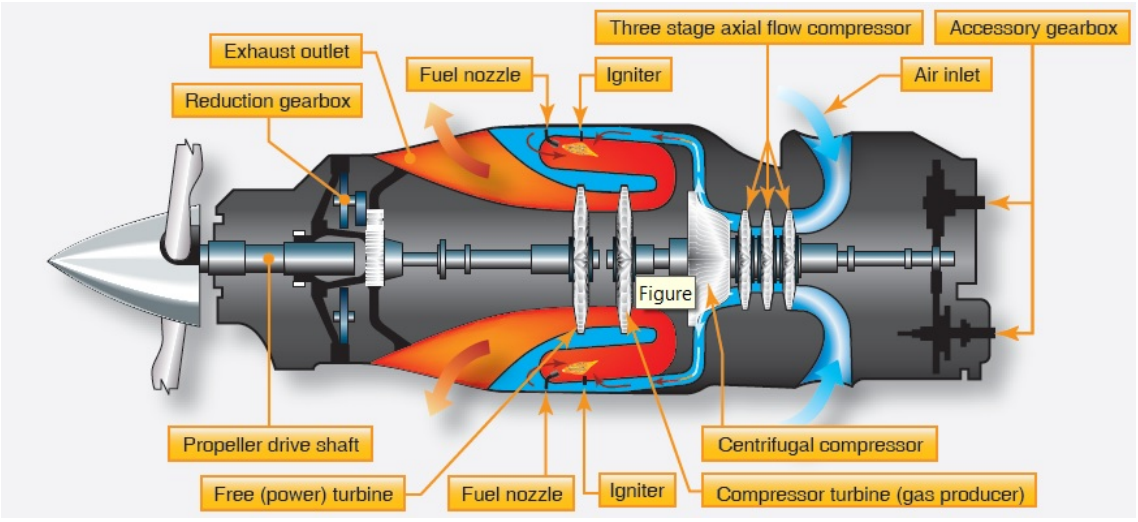

Figure 2.4 - Example of a split shaft/free turbine engine (Pratt & Whitney PT-6 engine). (FAA,2016)

2.2.1 Advantages and disadvantages of turboprop engines

The turboprop engines are usually used in small/medium airplanes for regional flights. Nevertheless, there are some exceptions which are cases of military cargo airplanes such as Airbus A400M. This last type of aircraft sometimes needs to operate in short runways and this type of engine allows them to do so comparatively to jet engines and they also have high power per unit of weight which allows them to carry more cargo at a higher efficiency level. The turboprop engines are also known for operating at lower altitudes compared to the other types of engines, and the propeller gives it a higher efficiency to operate at those levels. In case of engine failure, the propeller can be feathered to minimize drag, which is not possible for jet or turbofan engines. As they have relatively fewer parts moving during the operation, it has higher mechanical reliability. They are lightweight comparing to other types of engines, so they can provide better performance during takeoff while maintaining fuel efficiency. The turboprop engines have a most efficient performance when operating at speed between 250 and 400 mph and an altitude between 18000 and 30000 feet approximately (Skybrary, 2019).

However, there are not just advantages. At higher altitudes, the propeller loose efficiency and the vibration levels can cause some discomfort to passengers. En-route weather, such as turbulence or icing, can cause problems to the structures and additional passenger discomfort (Skybrary, 2019).

2.2.2 Components

The turboprop engine resides of three significant assemblages, the power section, the torque meter, and the reduction gear (Center for Naval Aviation Technical Training, 1991).

The power section assembly is the engine itself. This engine consists of an axial flow compressor, a combustion chamber, a turbine and accessory drive housing. The compressor shaft is extended to which the torque meter is attached.

The torque meter assembly is positioned between the power section and the reduction gear, and its purpose is to transfer and measure the shaft output from the power section to the reduction gear. This section is constituted by two concentric shafts. The inner shaft holds the load and produces the measured twist; meanwhile, the outer shaft is attached to the torque shaft at the drive input end only. There are separate extensions on both reference shafts and torque at the reduction gear assembly end. Rectangular exciter “teeth” are machined inline on each flange, which enables the pickups to detect the relative displacement of the two extensions. The housing of the torque meter serves as

rigid lower support between the power section and the reduction gearbox providing a mounting for the pickup assembly at the end of the reduction gearbox. This pickup assembly consists of electromagnetic pickups mounted radially over the “teeth” of the torque and reference shaft extensions and the produce electrical impulses at the passage of each exciter “tooth”. The signals are directed to the phase detection circuit of the torque meter indicator. This circuit controls the torque meter indicator, which registers the torque delivered into the reduction gear assembly. In short, the principal operation is measuring the angular deflection electronically (twist) that occurs in the torque shaft relative to the zero deflection of the reference shaft.

The reduction gear assembly converts high rpm, low torque of the turbine section in low rpm, high torque necessary for the efficient operation of the propeller. This assembly has an overall reduction gear ratio of about 13.5:1 accomplished in two stages, the sun and planet gears. The sun gear train allows the primary step-down, and the planet gear allows the secondary step-down. The reduction gear assembly includes safeties systems:

- Propeller brake.
- Negative torque system (NTS).
- Safety Coupling.
- Thrust sensitive signal system (TSS).

The propeller brake prevents the rotation of propeller when the engine is not operating, in case of feathering during the flight, and it helps to decrease the time to stop the propeller when the engine is shut down. It is located between the rear case and the inner diaphragm of the rear case and has three positions, locked, release and applied for positions. When the engine is running the pressure of the oil in the reduction gear assembly holds the brake in the release position keeping away the inner and outer members. The applied position takes in when the engine is shut down. During this operation, the oil pressure decreases and forces the contact of the inner and outer members. The propeller brake only locks when the propeller is moved in the opposite direction of a regular rotation (Center for Naval Aviation Technical Training, 1991).

The negative torque system prevents the propeller from driving the engine in a low power setting scenario and an appropriate airspeed for the airflow to cause an increase in the propeller rpm, and it limits undesirable torque resulting from this scenario. In short, it prevents the propeller from running the engine in case of excessive propeller drag when it is the engine that must drive the propeller, and it is prevented by controlling the pitch of the propeller blades (Center for Naval Aviation Technical Training, 1991).

The safety coupling is an automated device that prevents excessive propeller drag when the negative torque system is not running correctly and disconnects the power section from the reduction gearbox. It is at the end of the torque meter shaft that transmits the torque in the power section to the reduction gear assembly.

The thrust sensitive signal system is a device that feathers the propeller, in case of power loss, and shuts down the engine. By feathering the propeller, it is given a reduction in the yawing action and, in the case of multi-engine aircraft, there is a reduction in asymmetric flight characteristics.

2.2.2.1 Air inlet

The air inlet of a turboprop engine should be considered beyond the design factors. It should be taken in consideration the best inlet in terms of airflow and aerodynamics features, and it is necessary to keep in mind that many types of these engines are anti-iced by using electrical devices in the entrance of the intake. So, it is essential to take into consideration every element that affects, directly or indirectly, on the air inlet such as the propeller, driveshaft, the hub and the spinner.

The usual type of intake used in a turboprop engine is one single-bottom duct intake. However, there are other types as twin intake, curved intake and submerged intake. The twin intake air ducts usually are side-mounted and are used to lead the air to the compressor stage. It is usually a short-length duct which means a smaller drop in the pressure due to the less friction. The critical advantage in the submerged intake is the less drag and weight comparing to regular intake (F. El-Sayed, 2016).

2.2.2.2 Compressor

Two types of compressors can be used in a gas turbine engine, the axial and centrifugal. While the centrifugal compressor directs the fluid outward perpendicularly to the longitudinal axis, the axial compressor leads the airflow parallel to the rotational axis.

Both types of the compressors contain a rotating part, the rotor (impeller on centrifugal compressors), which transfers kinetic energy from the airflow as the air entering the compressor is slowing down and a static part, the stator (diffuser in centrifugal compressors), which redirects the airflow converting the kinetic energy of the airflow into pressure and slows down the fluid by increasing the flow area (Saravanamuttoo et al., 2006).

Axial flow compressors (see Figure 2.5) are the only ones used in large size engines because, for a given pressure and flow ratio, the frontal area is smaller, that is for the same mass flow, the diameter of an axial compressor would be smaller than a centrifugal compressor causing the engine weight to be lower as its diameter reduces. There is also a practical upper limit on the diameter of the centrifugal impeller (about 0.8 m) due to manufacturing difficulties which implies a limitation in the pressure ratio and mass flow capability.

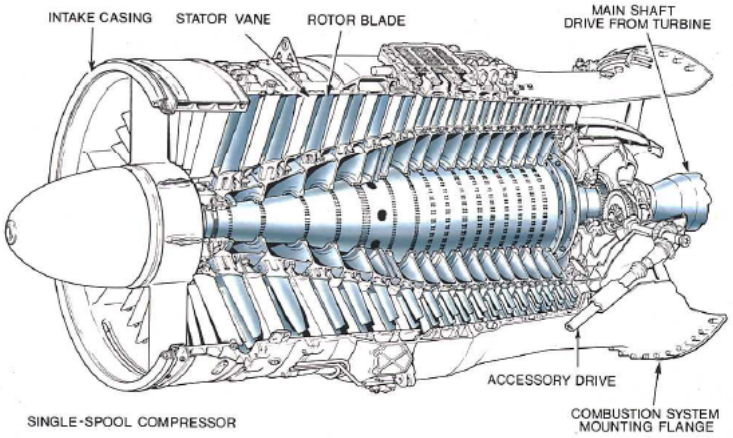

Figure 2.5 - Example of an axial flow compressor (From Rolls-Royce plc, The Jet Engine, 5th edition, Derby, U.K.,1996.)

For small size engines, the centrifugal compressors are most suitable. For a single-stage, the pressure ratio is higher (above 9:1) and for the same conditions would be needed more stages for an axial flow compressor, for a given pressure and flow ratio, the centrifugal compressor is shorter, and the Mach number on the exit of the compressor usually is lower, therefore, will be seen a decreasing in pressure loss through the downstream duct. The isentropic efficiency is better for lower mass flow ratios (less than 5kg/s) for the reason that for small axial flow compressors the tip clearance increases and there is manufacturing limitations for the blade leading and trailing edge thicknesses and surface roughness. This type of compressor is less susceptible to foreign object damage, and this susceptibility increases as the size of the compressor decrease. This because a centrifugal compressor (see Figure 2.6) consists in a “drum” with separate blades that can be replaced individually in case of damage instead of the all bladed disk that would be entirely replaced if damaged in an axial flow compressor. The individually replace leads to a reduction in unit cost (which is lower for the same mass flow and pressure ratios comparing to an axial flow compressor) and a decrease in manufacturing difficulties (El-Sayed, 2017).

This section is responsible for a variety of jobs beyond compressing the airflow before entering the combustion chamber. It is essential to remember that it is in this section that bleed air is extracted to air pressurization, air conditioning, turbine cooling and anti-icing devices on engine inlet.

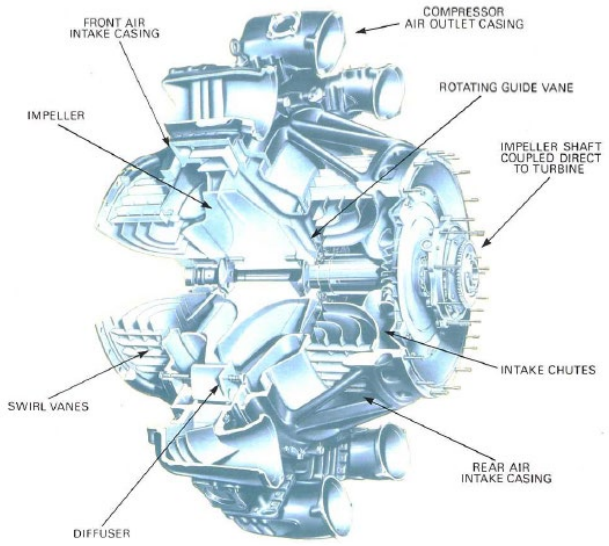

Figure 2.6 - Example of a centrifugal flow compressor (From Rolls-Royce plc, The Jet Engine, 5th edition, Derby, U.K.,1996.)

2.2.2.3 Combustion Chamber

The combustion chamber is the section of a turbine engine where the combustion of the fuel takes place. The compressor provides the air (compressed, heated and slowed down to the desired speed) to which fuel will be added and burned (Rolls-Royce, 1996). This combustion process needs activation energy that in this case, will be an electric spark, and it is only necessary for the combustion process initiation, once from then on, the flame must be self-sustaining.

There are many types of combustion chambers, and they can be categorized based on the combustion speed is subsonic or supersonic. Since turboprop engines are only for subsonic aircraft, more emphasis will be placed on the chambers for this type of aircraft despite all aircraft have subsonic combustors except for those who have scramjet engines. The main types of combustion chambers are tubular chamber (or can type), tubo-annular chamber and annular chamber.

The tubular combustion chamber (see Figure 2.7) consists of multiple tubes interconnected around the shaft between the compressor and the turbine. Although it can be used with both types of compressors (centrifugal and axial flow compressors), the

centrifugal compressor will be the most appropriate as the air is separated into equal portions to its outlet. Even though they have some advantages such as the easy replacement for maintenance, the desired air-fuel ratio is easily achieved, and only a small fraction of airflow is required for rig testing, the disadvantages are enough for taking this type of combustion chambers out of today's designs. Some of the disadvantages are high-pressure loss, high drag due to the large frontal area, huge, heavyweight; require interconnectors and experiences problems of light-round.

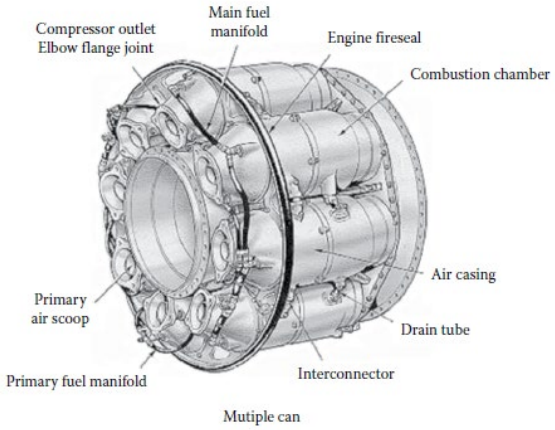

Figure 2.7 - Example of multiple combustion chamber. (From Rolls-Royce plc, The Jet Engine, 5th edition, Derby, U.K.,1996.)

The tubo-annular combustion chamber (can-annular or cannular) (see Figure 2.8) is like the tubular combustion chamber. The difference between them is that the multiple cylindrical burners are inside of an annulus that covers all the burner section. Besides, it is necessary to have fuel-drain valves in the bottom chambers to prevent from being burned at the next start.

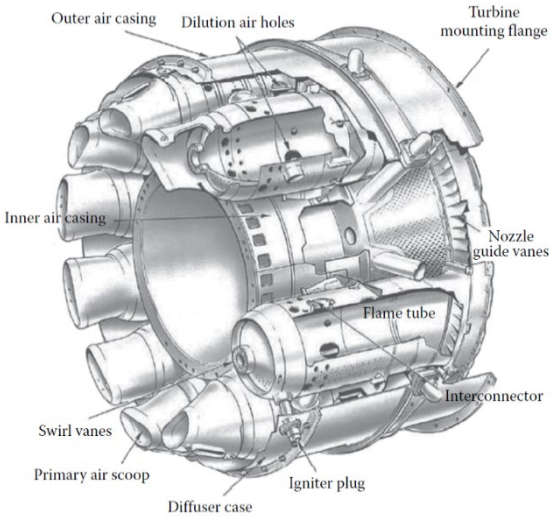

Figure 2.8 - Example of a Tubo-annular combustion chamber. (From Rolls-Royce plc, The Jet Engine, 5th edition, Derby, U.K.,1996.)

This type of combustion chamber overcomes some disadvantages of the tubular combustion chambers as they are shorter and lighter, and they have a low-pressure loss. However, they still require connectors, and they still incur problems of light around. The combustors that reverse flow during the combustion are usually tubo-annular.

The annular combustion chamber (see Figure 2.9) consists of an annular tube confined to an inner and outer casing (Rolls-Royce, 1996). They are used in most engines in aviation nowadays. Its aerodynamic configuration makes the combustion chamber smaller, leading to a decrease in weight and pressure loss. Comparing to a tubo-annular, the length is only 75% for the same diameter and for the same power output (which also means a reduction in production cost), the wall in contact with the combustion is much less, so it is required less 15% of the air to cool the wall to prevent the tube from burning. This air reduction leads to a reduction in air pollution too. Other advantages of this type of combustion chamber are:

- Less frontal area meaning less drag.
- Higher durability.
- Easy to manufacture due to the simplicity in the design.
- An easy mixture of fuel and air.
- Uniformity of the combustion zone.

Nevertheless, there are some disadvantages. When the maintenance comes, it is required to remove the engine from the aircraft, and for rig testing, it is necessary the full engine air mass flow. The match between airflow and fuel flow is difficult to achieve, and it is hard to keep stabilized the transverse outlet temperature (El-Sayed, 2017).

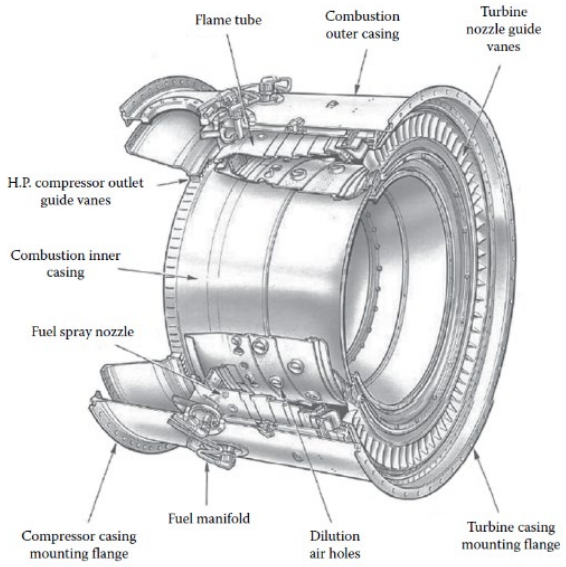

Figure 2.9 - Example of an Annular combustion chamber. (From Rolls-Royce plc, The Jet Engine, 5th edition, Derby, U.K.,1996.)

Components of the combustion chamber

Each type of combustion chamber has its components. I will focus on the tubo-annular combustion chamber once it is more complex than the annular, and it is like the tubular combustion chamber. The components of the tubo-annular combustion chamber are (El-Sayed, 2017):

- Case:

Removable shroud protected from the thermal load as the air flows in it.

- Diffuser:

The leading role of the diffuser is to optimize the high speed and pressurized air that exits the compressor for the combustor without a significant loss in pressure and flow separation.

- Liner:

As it will be exposed to long periods of high temperature due to combustion, the liner will have to be built to withstand them. That is the reason why they are usually made of superalloys or coatings that serves as thermal barriers. Due to the high temperatures in the combustion chamber, it is mandatory for the cooling of the liner, and there are two main types:

  - The film method, where the air injected from the outside (introduced through slats or louvers) creates a thin film layer of fresh air that will protect the liner and will reduce the temperature by almost a 1000K. However, the introduced air creates an irregular profile where the surface is not evenly cooled.
  - The transpiration method, where it is used a porous material that let in, uniformly, a small amount of cooling air (about 10% of the total airflow), resulting in an even temperature profile and a better performance of the combustion once less air is used for cooling.

- Snout

It is an extension of the dome, and the main function is to separate the primary airflow (needed for combustion) from the secondary airflow (used as cooling air).

- Dome/Swirler

The main task of this part of the engine is to create turbulence from the primary airflow to mix the air and the fuel quickly. It is essential to design this part cautiously in order to do not create more turbulence than is needed to the air/fuel mixture once this turbulence is created by a local low-pressure zone that forces some of the combustion products to recirculate, generating the high turbulence and higher the turbulence, higher the pressure loss in the combustion chamber.

- Fuel injector

As the name suggests, its primary purpose is to inject the fuel in the combustion chamber, and it is also responsible for mixing the fuel and the air. The main types of fuel injectors are

  - Airblast injector.
  - Premix/pre-vaporizing injector.
  - Pressure-atomizing injector.
  - Vaporizing injector.
  - Igniter

The electrical-spark igniters are the primary type used in gas turbine engines. Its location is inside the combustor far enough not to be damaged by the combustion but close enough to ignite the air/fuel mixture.

2.2.2.4 Turbine

The main task of the turbine is to convert the kinetic energy of the combustion gases from the combustor into mechanical energy (Kyprianidis et al., 2015) that will be used to drive the compressor and other accessories drives and, in case of the turboprop engines, provide the shaft power for a propeller. The turbine may have several stages of moving blades and stationary nozzle guide vanes depending on the connection among the power required from the gas flow, the rotational speed at which it must be produced and the diameter of the turbine allowed. It is required to keep in mind that aerodynamic takes a big part of the turbine and the nozzle guide vanes design since they are an airfoil shape. The number of turbines differs with the type of engine used, and it is related to the number of shafts used. In an engine with a high compression ratio, is typically used two shafts to drive the high and low compressors and, therefore, two turbines are needed to drive those shafts. In some cases of turboprop engines, the driving torque is given from a free-power turbine. This type of turbine is independent of the other turbine and compressor shafts, thus allowing it to run at its optimum speed.

There are three types of turbines:

- Impulse turbine.
- Reaction turbine.
- Impulse-reaction turbine.

The impulse turbine is built in single stage (having two or more turbines in the same shaft), and the blades generate a force in the fluid to change its momentum as the fluid generates a force in the blades that operates in the axis of rotation to create torque and force the rotors to move continuously. There is a drop in the pressure caused by the nozzle guide vanes due to their convergent shape and an increase in gas speed.

The reaction turbine is a type where there is no change in the pressure, and the nozzle guide vanes change the direction of the gas flow. As the name says, the spaces between the blades undergo a reaction force due to the gas flow expansion and acceleration.

The impulse-reaction turbine is a combination of both turbines mentioned above and the most common in gas turbines engines. The proportion of each principle is about 50% of impulsion and 50% of reaction, depending on the type of the engine.

Turbines may also be classified as axial flow turbines, radial flow turbines or mixed-flow turbines (a combination of both axial and radial turbines).

The axial turbines are the most common type used in gas turbine engines. They are designed to be highly efficient on big engines, with higher horsepower, lower fuel consumption and reduced noise. They are called axial turbine once the gas flow goes parallel to the axis of rotation.

In the radial turbines, the gas flow moves perpendicular while crossing the turbine.

As a mixed-flow turbine is a combination of both types of turbines, the gas flow moves both perpendicular and parallel to the axis of rotation.

2.2.2.5 Propelling Nozzle

The primary function of a propelling nozzle is to release the hot gases to the atmosphere and provide thrust. In the case of a turbo-propeller engine, the thrust produced by the propelling nozzle is almost despicable (null in some cases) once most of the power is absorbed by the turbine to drive the Propeller, the compressor and other accessories drives.

The design of the exhaust system is fundamental to the performance of the engine, in some cases, depending on the type of the gas turbine. This is because the turbine inlet temperature, the mass airflow as well as the velocity and pressure of the gases expelled are affected by some of the exhaust system characteristics as the jet pipe, outlet nozzle.

The basic types of nozzles in gas turbine engines are:

- Convergent nozzle.
- Convergent-divergent nozzle.

The convergent nozzle is the most common type used in subsonic flights (El-Sayed, 2016), and it is used if the nozzle pressure ratio is low. It is a simple convergent duct which suffers a decrease in cross-sectional area. In this duct, the mass airflow enters in a big section that gets smaller and, due to conservation of mass, it has to speed up in order to maintain a constant total of mass airflow moving in the smaller section. The energy to accelerate this fluid comes from the pressure. It is converted to streamflow, making the pressure drop.

The convergent-divergent nozzle is a combination of both ducts, respectively and it is used with a high nozzle pressure ratio (Mattingly, 1996), generally seen in supersonic aircraft.

In this type of nozzles, the hot gases expelled by the combustion chamber cross the turbine and converge to the throat (minimum area of the convergent duct) which is chosen to choke the mass airflow and set its rate through the exhaust system producing maximum thrust in case of isentropic expansion (Walsh & Fletcher, 2004). While the flow crosses the throat, the number of Mach is equal to one (sonic), and when it reaches the divergent part of the nozzle, the number of Mach becomes superior to one (supersonic). This transition to a supersonic state causes a drop in both temperature and static pressure.

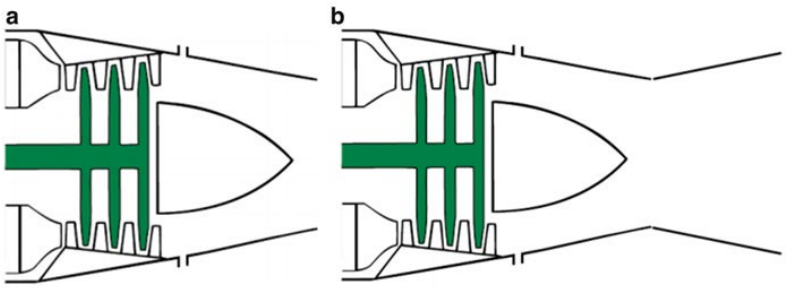

Figure 2.10 - Convergent (a) and convergent-divergent (b) nozzles (El-Sayed, Fundamentals of Aircraft and Rocket Propulsion)

To know the amount of impulse produced by the nozzle, it is required to know the outlet speed of the flow as well as its pressure and its outlet mass. The outlet speed is determined by the speed of sound, which in turn is determined by the outlet temperature. The transition to a supersonic state causes a drop in both static temperature and pressure, and the amount of supersonic expansion will determine the outlet temperature and pressure.

The nozzle may also be classified as:

- Fixed geometry type.
- Variable-geometry type.

The fixed-geometry type, as its name says, does not show any moving part or change its area and it is used in subsonic flight engines.

The variable-geometry type is used in engines with afterburners. The nozzle is reduced in the area, which leads to an increase in turbine inlet temperature and consequently an increase in exhaust velocity and thrust. There are three types of variable-geometry nozzles:

- Plug nozzle.
- Ejector type nozzle.
- Iris nozzle.

The plug type is a nozzle which incorporates a center body around which the fluid flows. The central *"plug employs an external expansion fan as the spike employs external oblique shocks"* (El-Sayed, 2017).

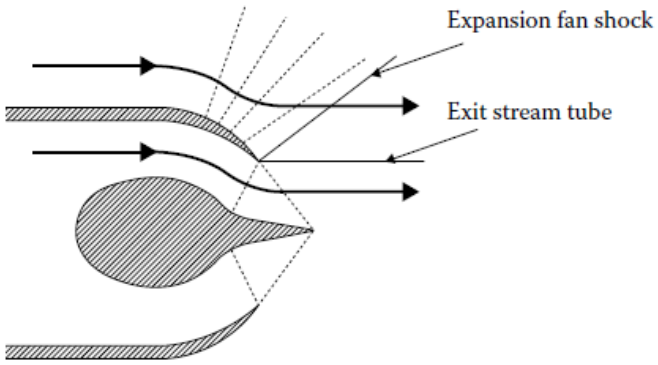

Figure 2.11 - Scheme of plug nozzle (Kerrebrock, J.L., Aircraft Engines and Gas Turbines, 1992)

The ejector nozzle uses a secondary airflow to create a capable nozzle. When the aircraft experience subsonic speeds the "spring-loaded petals" converge making the exhaust into a convergent type. As the aircraft speeds up, the nozzles open to a convergent-divergent type increasing the exit velocity of the gases. This type of nozzle is trustworthy, straightforward and have the ability to use de admitted air that is not used in the engine combustion, but it presents a high drag due to the secondary airflow, and its performance is average (Wikiwand, 2020).

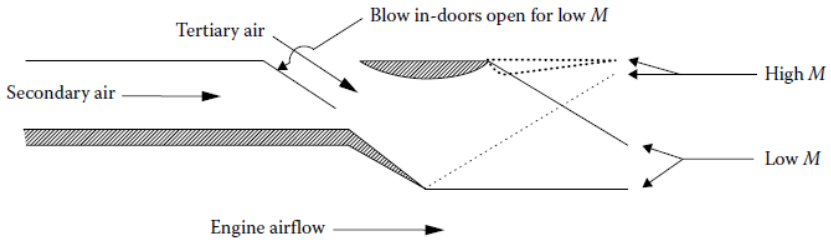

Figure 2.12 – Scheme of an ejector nozzle (Kerrebrock, J.L., Aircraft Engines and Gas Turbines, 1992)

The iris nozzle uses "*overlapping, hydraulically adjustable petals"* making this type much better at performance and smoother. Some of them may have the ability to change the angle of thrust (El-Sayed, 2016).

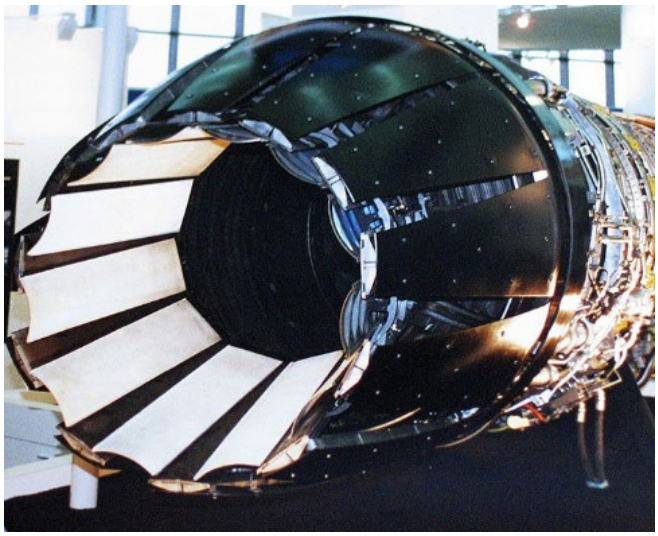

Figure 2.13 – Iris Nozzle (Wikiwand, 2020)

2.2.2.6 Propeller

Some aircraft use propellers (or a single propeller) to deliver thrust force. In a piston engine, the thrust produced by the propeller is 100% while it is responsible for delivering 80% - 90% of the thrust in a turboprop engine (10% to 20% of the propulsive force is produced by the jet).

Propellers have several definitions (El-Sayed, 2017) but, what comes to an aircraft propeller, it can be said that it is a fan or a device that have a central hub connected to the crankshaft of an engine with airfoil-shaped blades (with equal length) that converts rotational motion from piston engines or turboprops engines in thrust to pull or push the aircraft.

The propeller can have several classifications (El-Sayed, 2016).

Concerning their power source, they can be driven by piston engines or turboprop engines.

Regarding the material used in its construction, propellers can be made of wood, metal, aluminum alloy composite materials (fiberglass, for example).

About their coupling to the shaft, they can be classified as direct coupling or coupling by a gearbox unit.

Regarding control, they can be classified as fixed pitch, variable pitch, two-position propeller and adjustable pitch, constant-speed feathered and thrust reversal.

Propellers can also be classified according to the number of helices attached to each engine, single or counter-rotating.

About the propulsion method, they can be classified as pusher, puller or combination of both pusher and puller.

Propellers can also be classified by the number of blades (two, three, four and multiple - more than four).

Propellers components

Aircraft manufacturers are generally not responsible for propellers design. The propellers are manufactured by companies specialized in their design (Teeuwen, 2017).

The components of a propeller are (Center for Naval Aviation Technical Training, 1991): the blade that is composed by a blade back (surface seen when positioned in front of the propeller), blade face (surface seen when positioned in the back of the propeller), leading-edge (the edge in front when the blade is moving), the trailing-edge and the tip (the blade's part furthest from the hub).

the hub (central part to which the blades are attached).

the Shank (the thickened portion of the blade near the hub).

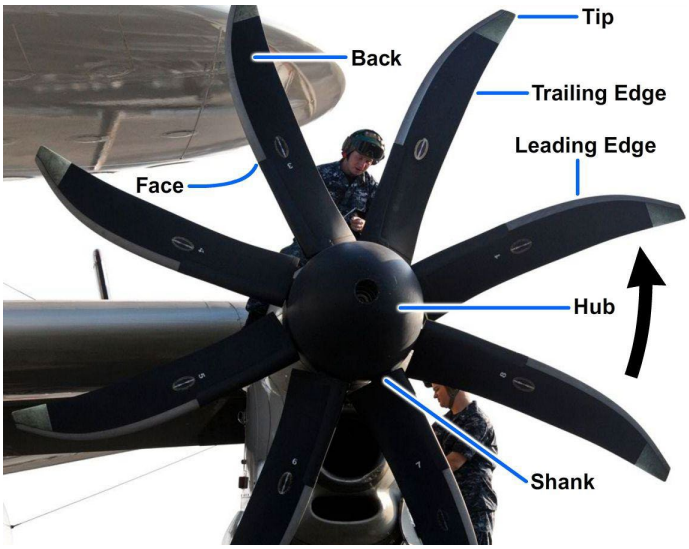

Figure 2.14 – Components of a propeller (NAVEDTRA, 1991)

Chapter 3

3. Methodology

It is required to know and follow the performance equations of the engine to be designed to achieve the design point of an engine. This chapter presents the performance equations used to design a two-spool turboprop engine as well as its design input data.

3.1 Design Point

For the calculation of a two-spool turboprop engine design point, was used the method that (Dinç, 2015) used to size a turboprop UAV and its propulsion system. To understand better the points from each parameter is calculated was used the following schematic (see Figure 3.1).

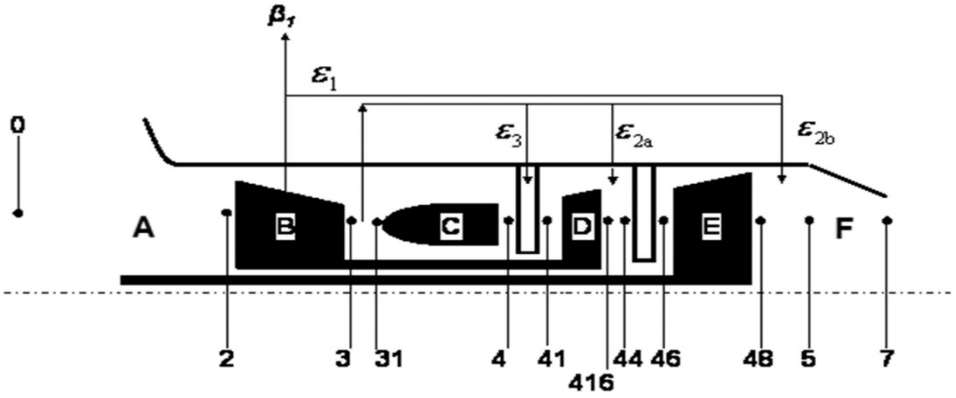

Figure 3.1 - Example of a schematic view of a two-spool turboprop engine (Walsh and Fletcher, 2004)

The main components of this engine are the intake (A), the compressor (B), the combustion chamber (C), the high-pressure turbine (D), low-pressure turbine (E) and the exhaust nozzle (F). The numbers represent the position of the parameter calculated related to each component.

3.1.1 Air Conditions

First, are calculated the stagnation temperature and stagnation pressure outside the intake given by the equations (3.1) and (3.2):

$$T_0 = Tamb * \left[1 + \left(\frac{\gamma - 1}{2}\right) * M^2\right] \quad (3.1)$$

$$P_0 = Pamb * \left[1 + \left(\frac{\gamma - 1}{2}\right) * M^2\right]^{\frac{\gamma}{\gamma-1}} \quad (3.2)$$

3.1.2 Intake

At intake, the temperature remains the same as external, but there may be a loss of total pressure depending on the design input:

$$T_{02} = T_0 \quad (3.3)$$

$$P_{02} = P_0 * (1 - \Delta Pin) \quad (3.4)$$

3.1.3 Compressor

3.1.3.1 Compressor Section

The intake leads to the compressor section, that, in order to know the stagnation temperature and stagnation pressure right after the section, one needs to calculate the isentropic efficiency:

$$\eta 2 = \frac{(\Pi c)^{\frac{\gamma c-1}{\gamma c}} - 1}{(\Pi c)^{\frac{\gamma c-1}{\gamma c * \eta c,pol}} - 1} \quad (3.5)$$

$$T_{03} = T_{02}\left(1 + \frac{1}{\eta 2} * \left(\Pi c^{\frac{\gamma-1}{\gamma}} - 1\right)\right) \quad (3.6)$$

$$P_{03} = P_{02} * \Pi c \quad (3.7)$$

3.1.3.2 Compressor Exit Airflow

The airflow rate at the inlet of the compressor is a design parameter. However, there may be a decrease if there is air to be used for cooling the low-pressure turbine.

$$\dot{m}3 = \dot{m}2 - \dot{m}2 * (\beta 1 + \varepsilon 1) \tag{3.8}$$

$$Tbleed = \frac{T_{03} + T_{02}}{2} \tag{3.9}$$

With the knowledge of the airflow rate and the compressor middle stage stagnation temperature, the power required for the compressor can be estimated:

$$Gc = \dot{m}3 * Cpc * (T_{03} - T_{02}) + (\dot{m}2 - \dot{m}3) * Cpc * (Tbleed - T_{02}) \tag{3.10}$$

3.1.3.3 Compressor Exit Diffuser

At the compressor exit diffuser, the stagnation temperature and pressure remain the same. However, the air mass flow may be reduced due to bleed and cooling air extraction for the high and low-pressure turbine and nozzle guide vanes:

$$T_{031} = T_{03} \tag{3.11}$$

$$P_{031} = P_{03} \tag{3.12}$$

$$\dot{m}31 = \dot{m}3 - \dot{m}2 * (\varepsilon 2a + \varepsilon 2b + \varepsilon 3) \tag{3.13}$$

3.1.4 Combustion Chamber and NGV Station

At the combustion chamber, the pressure loss is:

$$P_{04} = P_{031} * (1 - \Delta Pb) \tag{3.14}$$

For the fuel-air ratio calculation:

$$f1 = 0.10118 + (2.00376 * 10^{-5}) * (700 - T_{031}) \tag{3.15}$$

$$f2 = 3.7078 * 10^{-3} - (5.2368 * 10^{-6}) * (700 - T_{031}) - (5.2632 * 10^{-6}) * T_{04} \tag{3.16}$$

$$f3 = (8.889 * 10^{-8}) * |T_{04} - 950| \tag{3.17}$$

$$f = \frac{\left(f1 - (f1^2 + f2)^{\frac{1}{2}} - f3\right)}{\eta b} \tag{3.18}$$

Knowing the fuel-air ratio is now possible to calculate the fuel flow and therefore, the total mass flow after the combustion:

$$\dot{m}f = f * (\dot{m}31 + \dot{m}2 * \varepsilon 3) \tag{3.19}$$

$$\dot{m}4 = \dot{m}31 + \dot{m}f \tag{3.20}$$

However, the total mass flow may be different at the inlet of the turbine if there is a mass flow used to cool the nozzle guide vanes:

$$\dot{m}41 = \dot{m}31 + \dot{m}2 * \varepsilon 2 + \dot{m}f \tag{3.21}$$

The stagnation temperature at the inlet of the turbine will depend on a design input which is the stagnation temperature at the exit of the combustion chamber:

$$T_{041} = \frac{\dot{m}4 * Cpt * T_4 + \dot{m}2 * \varepsilon 3 * Cpc * T_{031}}{\dot{m}41 * Cpt} \tag{3.22}$$

If it is assumed that there is not a pressure loss at the nozzle guide vane, the stagnation pressure remains the same:

$$P_{041} = P_4 \tag{3.23}$$

3.1.5 Turbine

3.1.5.1 High-Pressure Turbine

The high-pressure turbine will be used to drive the compressor. Assuming its mechanical efficiency, one can calculate the power extracted by the high-pressure turbine and consequently the temperature after crossing that section:

$$Ghpt = \frac{Gc}{\eta m} \tag{3.24}$$

$$T_{0461} = T_{041} - \frac{Ghpt}{(\dot{m}41 * Cpt)} \tag{3.25}$$

In order to determine the high-pressure turbine isentropic efficiency, it is necessary to assume an initial value for the stagnation pressure ratio of the turbine. Then, the two equations (3.26 and 3.27) may be iterated the needed number of times until they converge to a value that will be assumed as the isentropic efficiency.

$$\eta 416 = \frac{1 - \Pi t^{\frac{(1-\gamma t)\eta t,pol}{\gamma t}}}{1 - \Pi t^{\frac{1-\gamma t}{\gamma t}}} \tag{3.26}$$

$$\Pi t = \frac{e^{\log\left(1-\frac{T_{041}-T_{0461}}{\eta 416 * T_{041}}\right)}}{\frac{1-\gamma t}{\gamma t}} \tag{3.27}$$

To estimate the stagnation pressure at this point will be used the new value of the stagnation pressure ratio given by the equations (3.26) and (3.27):

$$P416 = \frac{P_{04}}{\Pi t} \tag{3.28}$$

There is no change in the total airflow mass:

$$\dot{m}416 = \dot{m}41 \tag{3.29}$$

Rotor cooling air addition is done numerically at station 44 (Kurzke, 2007), so the total airflow may suffer an increase:

$$\dot{m}44 = \dot{m}416 + \dot{m}2 * \varepsilon 2a \tag{3.30}$$

$$T_{044} = \frac{(\dot{m}416 * Cpt * T_{0416} + \dot{m}2 * \varepsilon 2a * Cpc * T_{031})}{\dot{m}44 * Cpt} \tag{3.31}$$

$$P_{044} = P_{0416} \tag{3.32}$$

3.1.5.2 Turbine Duct (between HPT and LPT)

At the duct between the high-pressure turbine and low-pressure turbine, there is no variation of the stagnation temperature and airflow, but the stagnation pressure may be reduced:

$$T_{046} = T_{044} \tag{3.33}$$

$$P_{046} = P_{0416} * (1 - \Delta Pt, duct) \tag{3.34}$$

$$\dot{m}46 = \dot{m}44 \tag{3.35}$$

3.1.5.3 Low-Pressure Turbine

In order to estimate the stagnation pressure after the low-pressure turbine, we need to calculate the pressure at the exhaust nozzle inlet, which will depend on the exhaust nozzle pressure ratio (design input):

$$P_{05} = \Pi n * Pamb \tag{3.36}$$

$$P_{048} = \frac{P_{05}}{1 - \Delta Pj, pipe} \tag{3.37}$$

Then, to calculate the stagnation temperature outside the LPT, it is necessary to estimate the isentropic efficiency for LPT:

$$\eta 46 = \frac{1 - \Pi t^{\frac{(1-\gamma t)\eta t, pol}{\gamma t}}}{1 - \Pi t^{\frac{1-\gamma t}{\gamma t}}} \tag{3.38}$$

$$T_{048} = T_{046} * \left(1 - \eta 46 * \left(1 - \Pi t^{\frac{1-\gamma t}{\gamma t}}\right)\right) \tag{3.39}$$

The power generated by LPT which will be used to drive the Propeller and the accessories drives is estimated by:

$$Glpt = (T_{046} - T_{048}) * (\dot{m}46 * Cpt) \tag{3.40}$$

That gives the engine shaft power:

$$PW = Glpt * \eta m \tag{3.41}$$

3.1.5.4 Low-Pressure Turbine Exit

The total airflow may change while crossing the LPT if there is air extraction at the compressor middle stage to cool the LPT:

$$\dot{m}48 = \dot{m}46 \tag{3.42}$$

$$\dot{m}5 = \dot{m}48 + \dot{m}2 * \varepsilon 1 + \dot{m}2 * \varepsilon 2b \tag{3.43}$$

$$T_{05} = \frac{\dot{m}48 * Cpt * T_{048} + \dot{m}2 * \varepsilon 1 * Cpc * Tbleed + \dot{m}2 * \varepsilon 2b * Cpc * T_{031}}{\dot{m}5 * Cpt} \tag{3.44}$$

3.1.6 Exhaust Nozzle

At the exhaust nozzle stage, there is no change of the stagnation temperature and airflow, so:

$$T_{07} = T_{05} \tag{3.45}$$

$$\dot{m}7 = \dot{m}5 \tag{3.46}$$

However, there is a change in the stagnation pressure, and it is necessary to know whether the nozzle is choked or not.

To know this condition, one needs to estimate the nozzle pressure ratio in a choked condition which is given by equation (3.47):

$$\frac{P5}{P7s, c} = \left(\frac{1 + \gamma c}{2}\right)^{\frac{\gamma c}{\gamma c - 1}} \tag{3.47}$$

If the exhaust nozzle pressure ratio (design input), Πn, is higher than $P_{05}/P_{7s,c}$, the nozzle is choked, and M7 is equal to 1.

The exit static conditions of the choked nozzle are:

$$T7s,c = \frac{T_{05}}{1+\frac{\gamma t-1}{2}} \tag{3.48}$$

$$a7 = (\gamma t * R * T7s,c)^{\frac{1}{2}} \tag{3.49}$$

$$A7,c = \frac{0.001 * \dot{m}5}{Ncd * (\frac{P5}{T5^{\frac{1}{2}}}) * (\frac{\gamma t}{R})^{\frac{1}{2}} * \left(\frac{\gamma t+1}{2}\right)^{\frac{-\gamma t-1}{2*(\gamma t-1)}}} \tag{3.50}$$

$$Fa = \dot{m}5 * a7 + A7,c * Ncd * (P7s,c - Pamb) * 1000 \tag{3.51}$$

If $P_{05}/P_{7s,c}$ is higher than Πn, the nozzle is not chocked, and the Mach number is not 1, the static temperature and the speed at the exit of the nozzle as well as the nozzle thrust can be calculated by equations (3.52) to (3.55):

$$M7 = \left(\frac{2}{\gamma t-1} * \left(\left(\frac{Pamb}{P5}\right)^{\frac{1-\gamma t}{\gamma t}} - 1\right)\right)^{\frac{1}{2}} \tag{3.52}$$

$$T7s = \frac{T_{05}}{1+\frac{\gamma t-1}{2} * M7^2} \tag{3.53}$$

$$a7 = (\gamma t * R * T7s)^{\frac{1}{2}} \tag{3.54}$$

$$Fa = \dot{m}7 * a7 * M7 \tag{3.55}$$

3.1.7 Propeller Thrust Calculation

For propeller thrust, is needed the knowledge of its advance ratio, power and thrust coefficient:

$$J = \left(\frac{V0}{n}\right) * d \tag{3.56}$$

$$Cpw = \frac{PW}{n^3 * d^5 * \rho} \tag{3.57}$$

$$Cf = \frac{\eta prop, d * Cpw}{J} \tag{3.58}$$

For static condition (V0=0):

$$Cf = (\eta prop, s * Cpw)^{\frac{2}{3}} * (\frac{\pi}{2})^{\frac{1}{3}} \tag{3.59}$$

$$Fp = \frac{Cf * PW}{Cpw * n * d} \tag{3.60}$$

3.1.8 Total Thrust and Specific Fuel Consumption

To estimate the total thrust and specific fuel consumption:

$$V0 = M0 * (\gamma c * R * Tamb)^{\frac{1}{2}} \tag{3.61}$$

$$Fnet = Fp + Fa * Ncx - \dot{m}2 * V0 \tag{3.62}$$

$$TSFC = \frac{\dot{m}f}{Fnet} \tag{3.63}$$

$$PSFC = \frac{\dot{m}f}{PW} \tag{3.64}$$

$$EPW = PW + \frac{V0 * Fa}{\eta p} \tag{3.65}$$

$$ESFC = \frac{\dot{m}f}{EPW} \tag{3.66}$$

The performance codes of an engine require some data inputs of installed thrust and fuel flow that may not be available by the engine company and to generate them can take a very long time (Chaput, 2010). So, some of the variables had to be assumed by other micro gas turbine engines. For this design point, the data assumed is presented in Table 3.1.

Table 3.1 - Engine and Propeller parameters assumed

Engine and Propeller Parameters	*Value*
Tamb	288.15
Pamb [kpa]	101.325
ΔPin	0
Πc	[2.08 – 10.08]
ηc,pol	0.795
$\dot{m}$2 [kg/s]	[0.1145, 0.1445, 0.1745, 0.2045]
β1	0
ε1	0
ε2a	0.05
ε2b	0
ε3	0.05
ΔPb	0.03
T4	[900 - 1200]
ηb	0.999
ηm	0.995
Πt	0.86
ηt,pol	0.86
ΔPt,duct	0.025
Πn	1.8
ΔPj,pipe	0.02
n	1200
d	0.3
ηprop,d	0.8
ηprop,s	0.7
Ncx	0.99
ηp	0.85

Chapter 4

4. Parameter Study

This parametric study intends to observe the behavior of some parameters by varying independent parameters and understanding the relationship between them.

In this way, the independent parameters to be varied are the altitude, constant flight speed, airflow at the intake, total pressure ratio in the compressor and turbine inlet temperature to verify later the behavior of the ESFC, TSFC, PSFC EPW and Fnet (dependent parameters) and the relationship between them.

4.1 Altitude Effect

With the increase in altitude, some properties change, the temperature, pressure and air density that, in a way, influences the work of the engine components, the turbine, responsible for providing energy.

By analyzing Figure 4.1, can be seen that the ESFC decreases with increasing altitude and the most significant decline is obtained up to 600 meters in altitude and, from that altitude, it becomes a little more constant. This decrease in ESFC is due to the decline in temperature with increasing altitude. These air properties influence the ESFC since the admitted airflow influences it.

The variation of the EPW according to the altitude (Fig. 4.1) sees a more significant increase up to 1000 meters, approximately being that, from that altitude, the growth becomes a little more constant. EPW is influenced by PW, which in turn is affected by temperature and airflow, Fa and flight speed. So, we can see that the EPW increases with altitude and its maximum value correspond to the maximum altitude of this study.

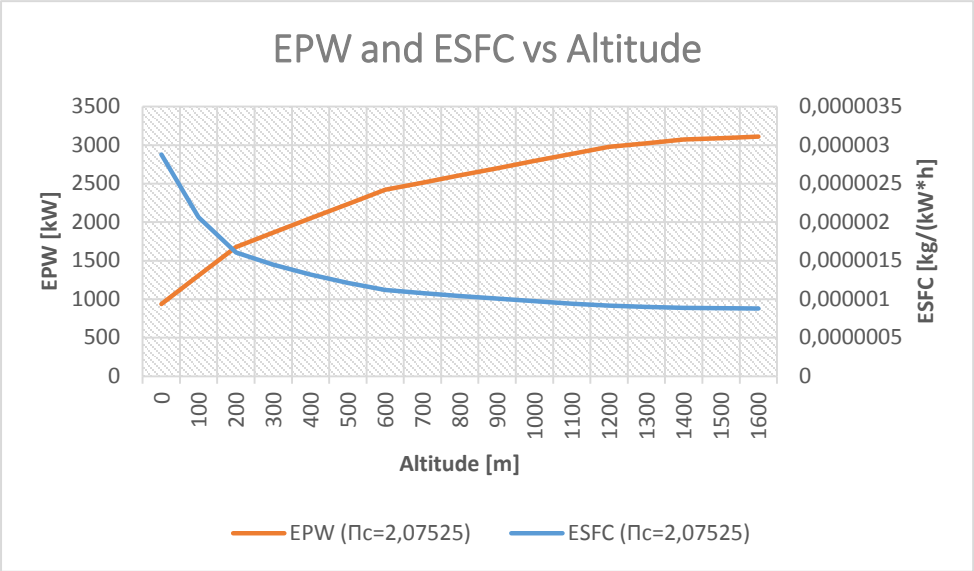

Figure 4.1 - Effect of altitude on EPW and ESFC

Fnet is a parameter that is influenced by the propulsive force of the Propeller and nozzle, the airflow, and the aircraft flight speed. In turn, thrust is related to air properties that vary with altitude (decrease in temperature, pressure, and air density). Through figure 4.2, it is possible to conclude that the Fnet decreases with altitude, and this decrease becomes less evident near the maximum height of this study.

TSFC is a parameter influenced by the fuel flow as a function of total net thrust. It is possible to observe that, as the altitude increases, the TSFC also increases. This increase happens since TSFC is inversely proportional to Fnet, so if this last parameter decreases, the thrust specific fuel consumption increases.

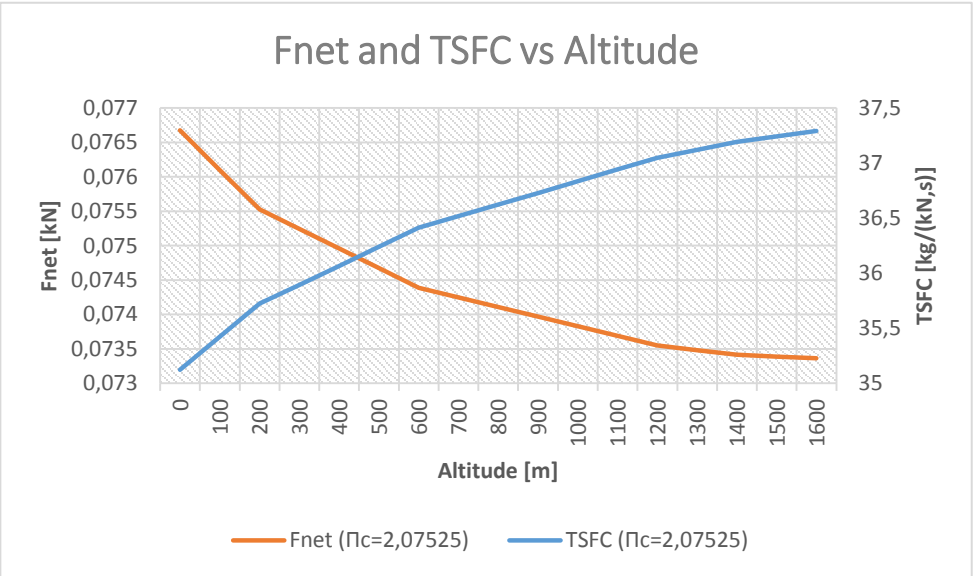

Figure 4.2 - Effect of altitude on Fnet and TSFC

PSFC is a parameter that relates the fuel flow as a function of the engine shaft power. Through figure 4.3, we can see that the PSFC increases with altitude. This increase happens since, although the engine shaft power increases (which would lead us to predict a decrease in PSFC) the increase in fuel flow with altitude is more significant.

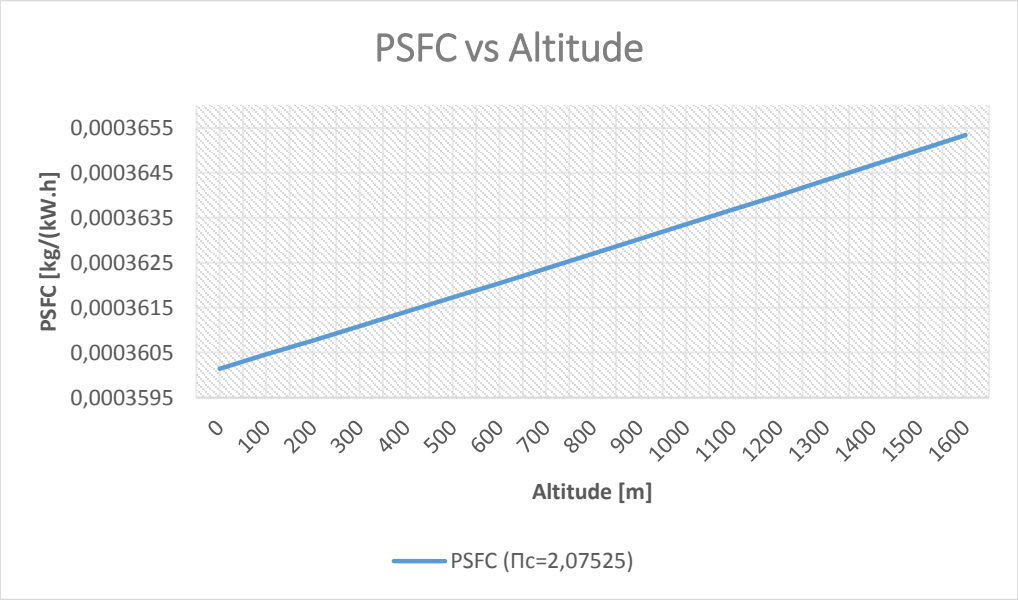

Figure 4.3 - Effect of altitude on PSFC

4.1.1 Effect of Altitude with Compressor Total Pressure Ratio Variation

Figures 4.4 and 4.5 show the effect of altitude with a compressor total pressure ratio variation on ESFC and EPW, respectively. One can see that the change in the pressure ratio in the compressor causes a subtle variation in the ESFC. However, this does not happen in EPW. Although it is not a considerable variation, we can observe that the increase in the total pressure ratio in the compressor decreases the power of the shaft in the engine. This drop is because despite the increase in compressor total pressure ratio, increasing the power generated by HPT and LPT will decrease the nozzle thrust, subsequently causing a decrease in EPW.

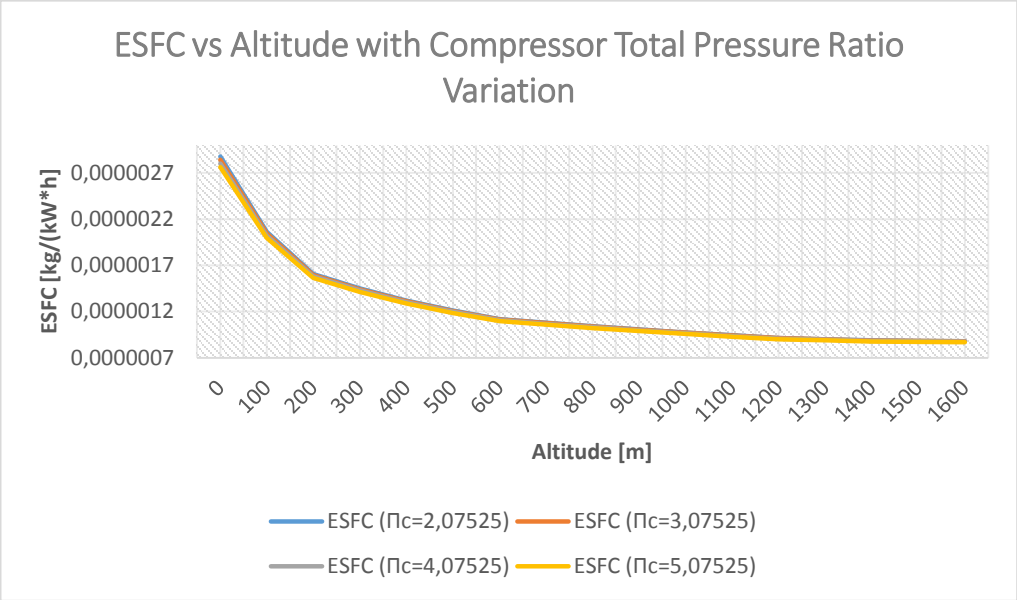

Figure 4.4 - Effect of Altitude on ESFC with Compressor Total Pressure Ratio Variation

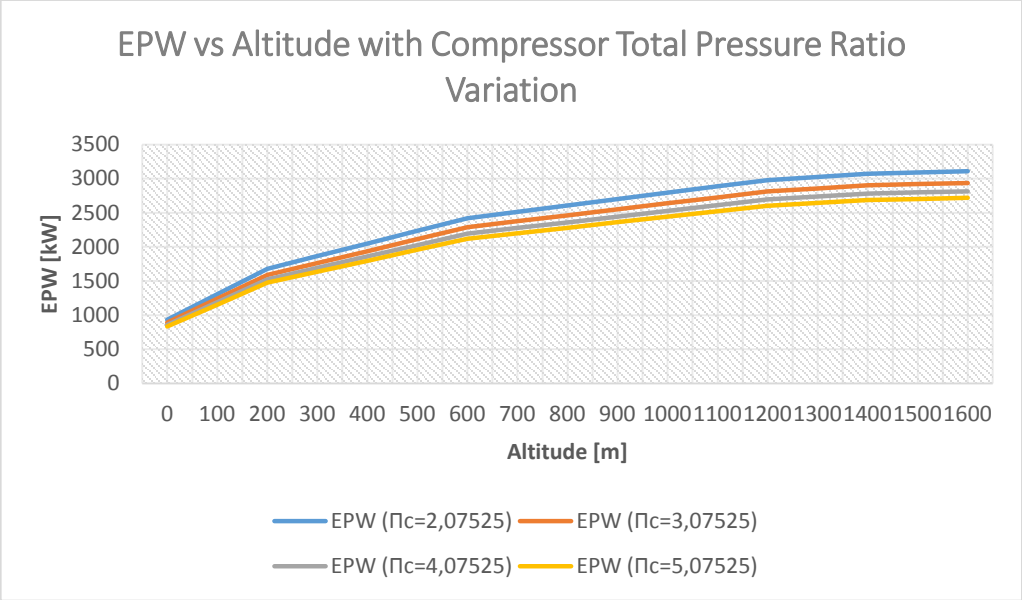

Figure 4.5 - Effect of Altitude on EPW with Compressor Total Pressure Ratio Variation

Through the analysis of figure 4.6, it is possible to verify that the change of TSFC with the variation of the compressor total pressure ratio is very subtle and that the TSFC decreases to higher altitudes. This variation is due to the decrease in Fnet with the increase in compressor total pressure ratio. This variation is more evident through the analysis of figure 4.7, where the increase in compressor total pressure ratio causes a decrease in total net thrust.

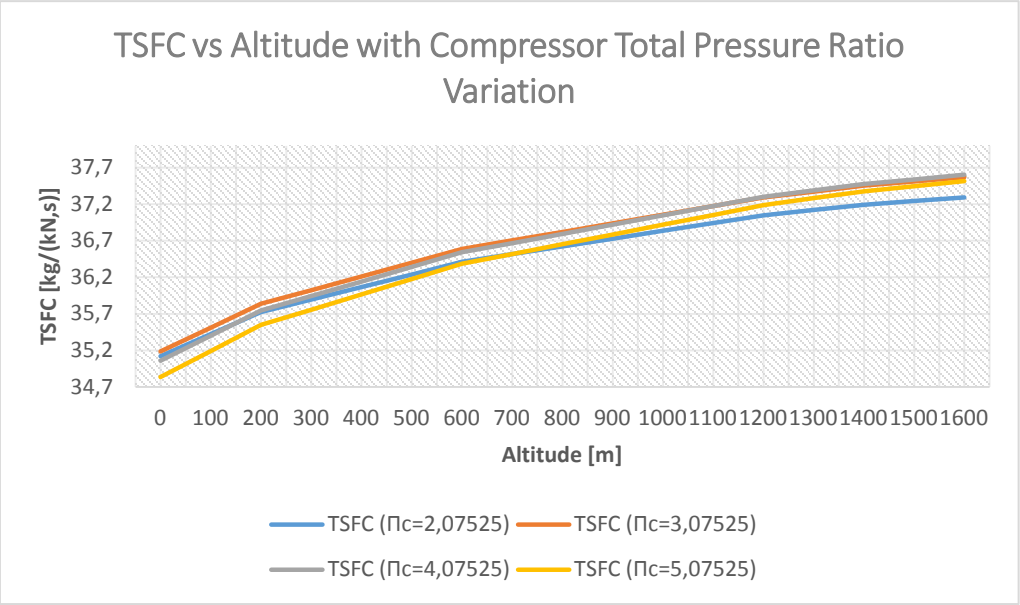

Figure 4.6 - Effect of Altitude on TSFC with Compressor Total Pressure Ratio Variation

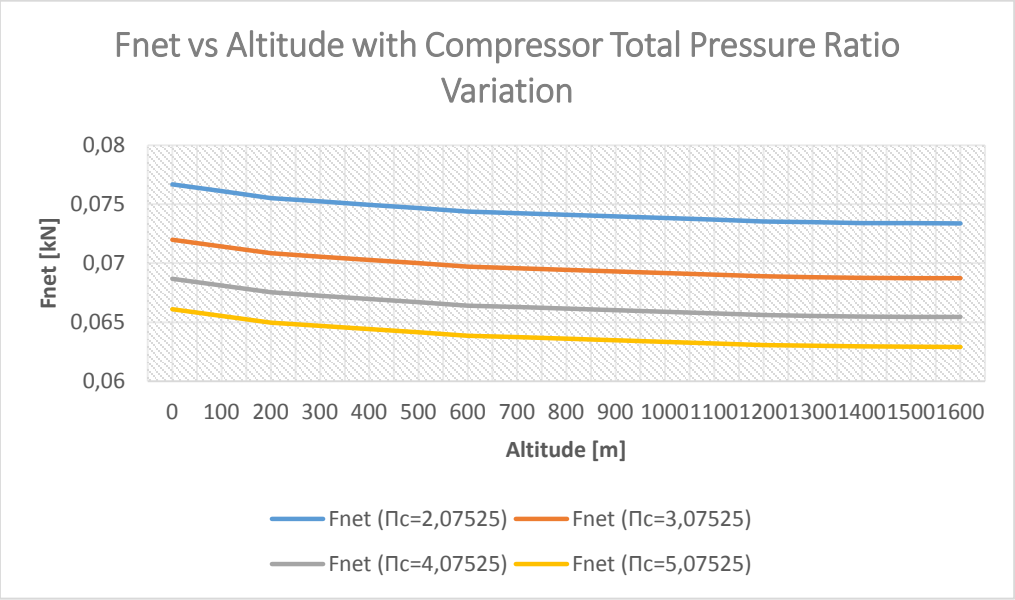

Figure 4.7 - Effect of Altitude on Fnet with Compressor Total Pressure Ratio Variation

The analysis in figure 4.8 shows such a small increase in PSFC with increasing altitude that it seems constant. However, we can see that the rise in CTPR leads to a decrease in PSFC verifying the most significant variation between the compression ratio of 2.07525 and 3.07525.

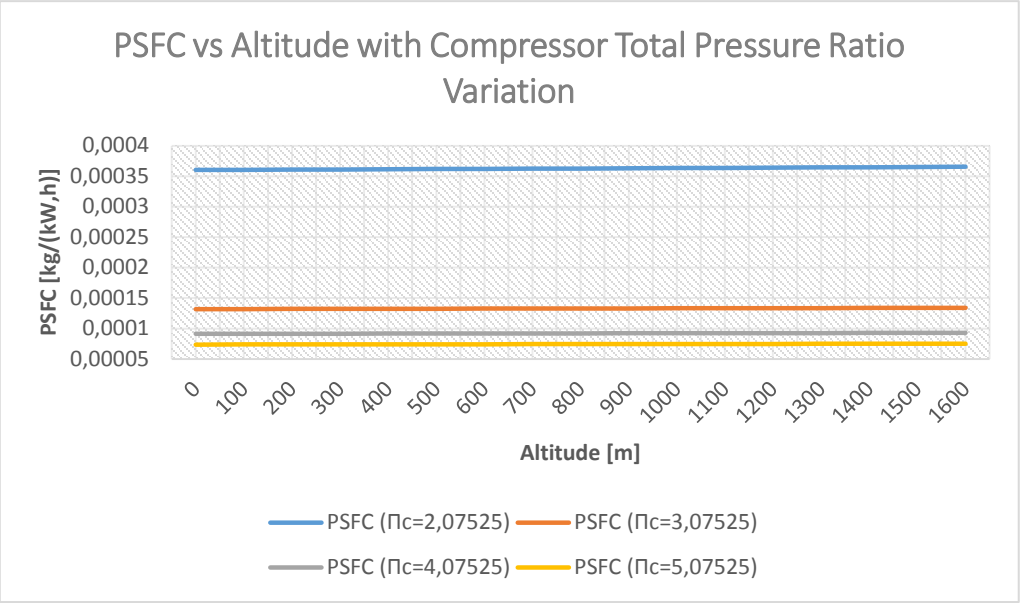

Figure 4.8 - Effect of Altitude on PSFC with Compressor Total Pressure Ratio Variation

4.2 Engine Airflow at Intake Effect

Figure 4.9 shows us that the variation of the airflow at the intake does not have much influence on the ESFC since the alteration is minimal. However, through figure 4.10, we can see that it has a significant impact on EPW. The increase in the airflow at the intake causes an increase in EPW with increasing altitude, and this difference is more visible as the altitude increases.

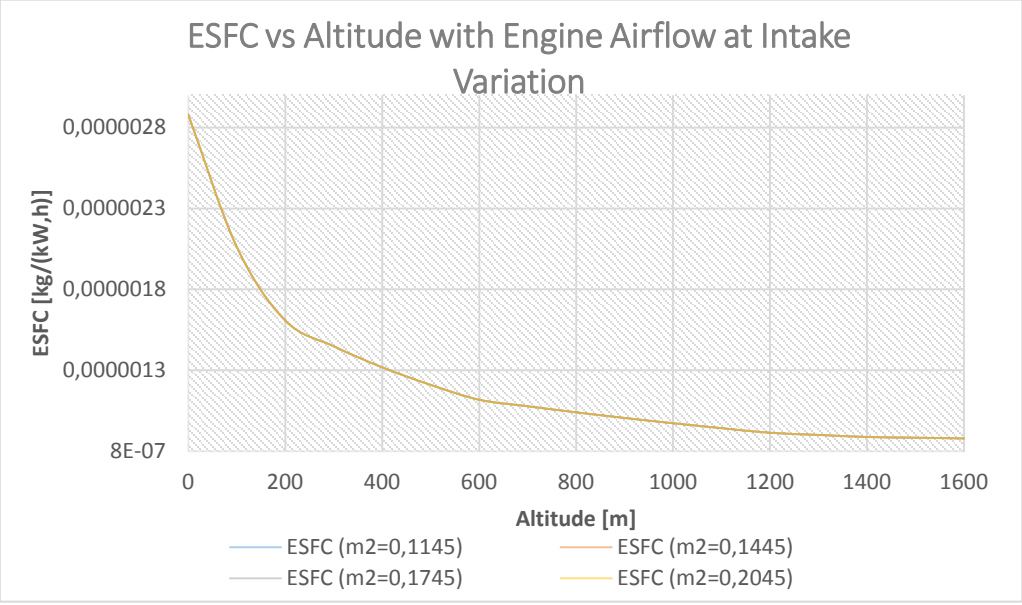

Figure 4.9 - Effect of Altitude on ESFC with Engine Airflow at Intake Variation

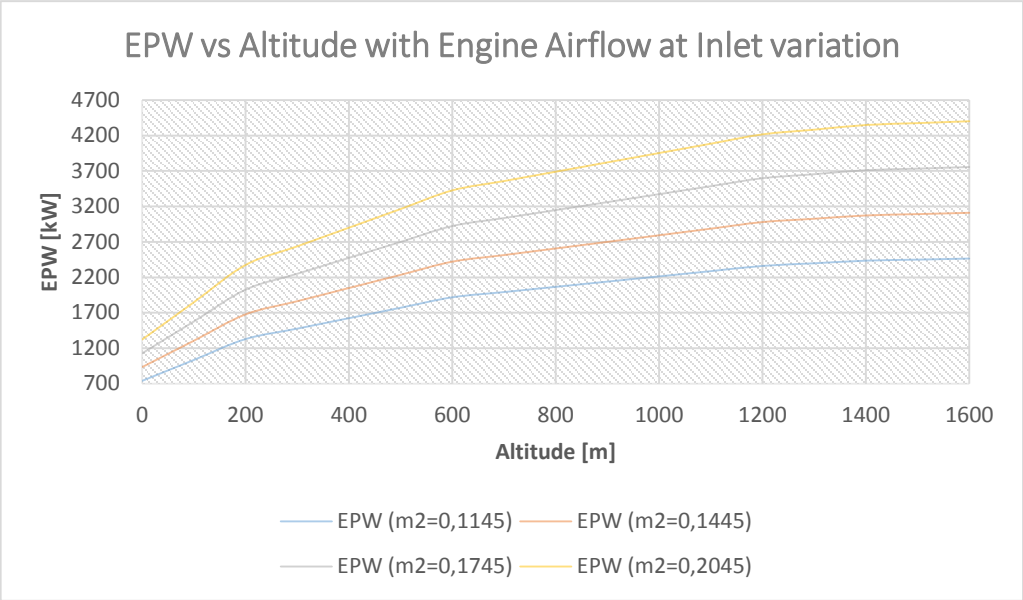

Figure 4.10 - Effect of Altitude on EPW with Engine Airflow at Intake Variation

It is noticeable through the analysis of figure 4.11 that the increase in the airflow at the intake does not affect the TSFC. On the other hand, it is possible to verify (figure 4.12) that the rise in the airflow leads to an increase in power that decreases as the altitude increases.

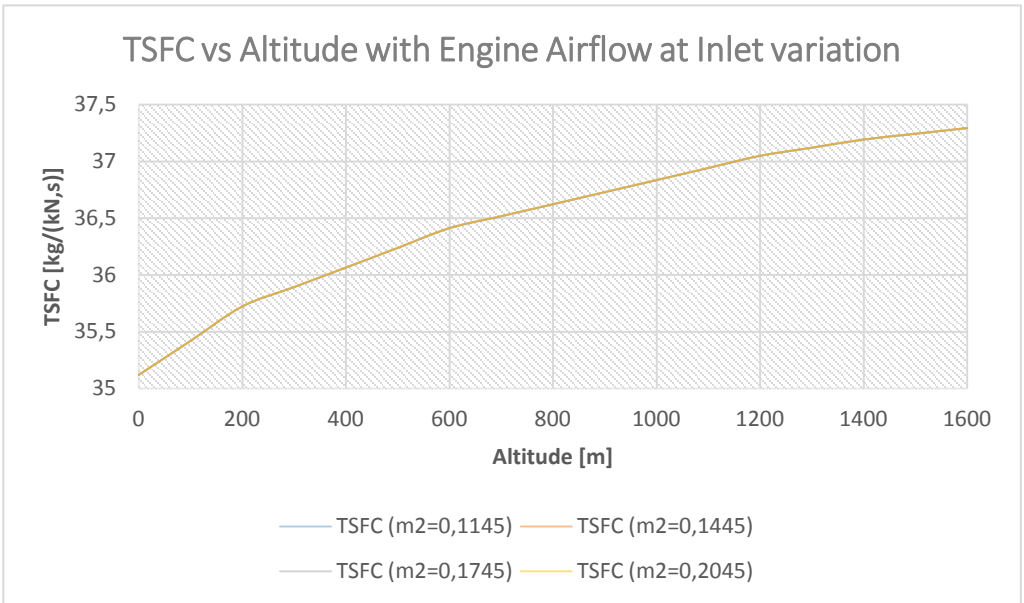

Figure 4.11 - Effect of Altitude on TSFC with Engine Airflow at Intake Variation

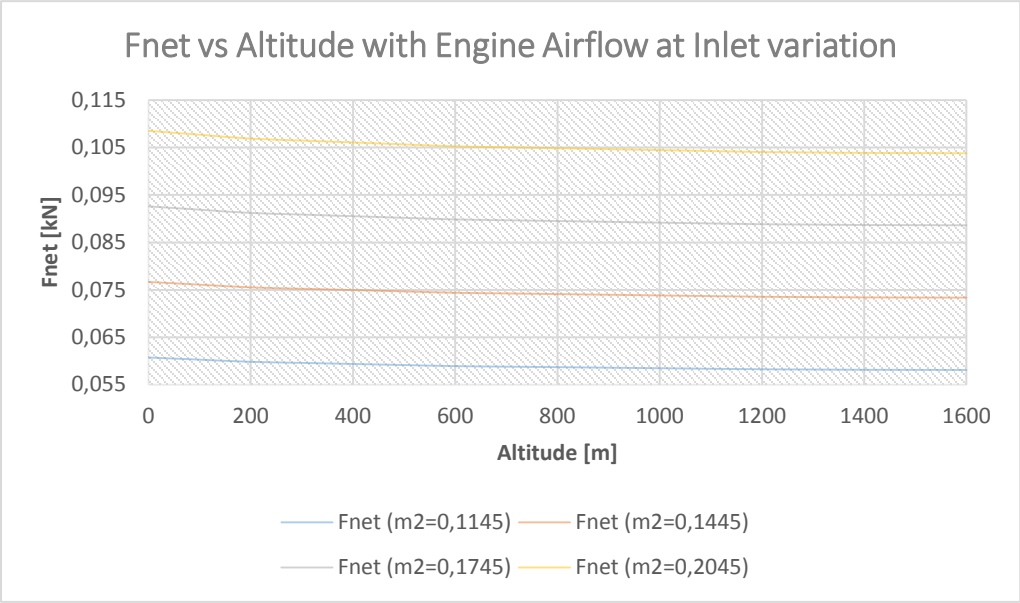

Figure 4.12 - Effect of Altitude on Fnet with Engine Airflow at Intake Variation

Through figure 4.13, it is possible to observe that the PSFC increases with the increase in altitude without any significant effect with the rise in the airflow at intake.

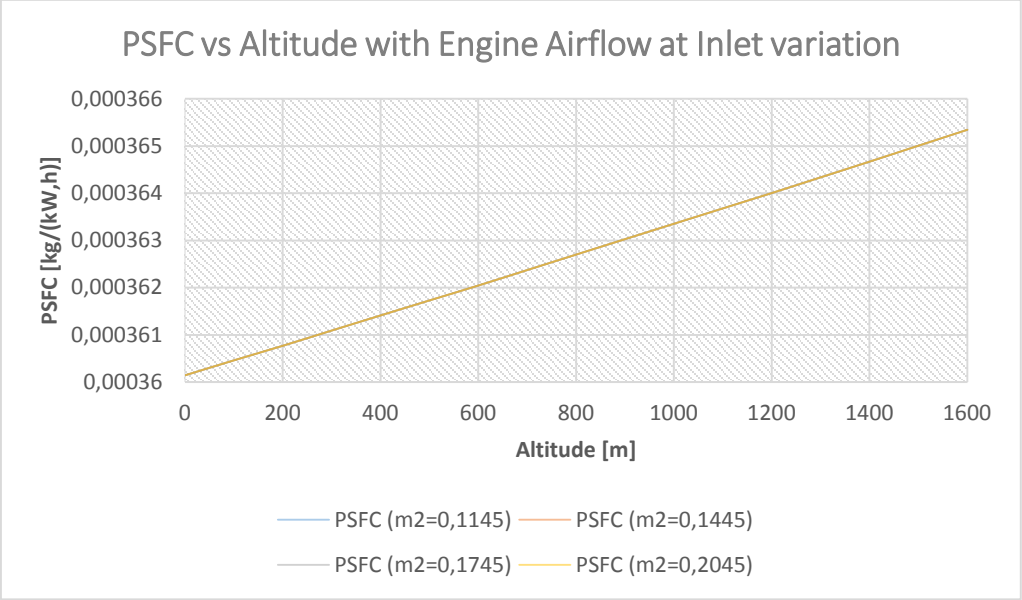

Figure 4.13 - Effect of Altitude on PSFC with Engine Airflow at Intake Variation

4.3 Compressor Total Pressure Ratio Effect

An analysis of figure 4.14 shows that the ESFC decreases with the increase in the CTPR; this decrease is more accentuated for the pressure ratio between 2.07525 and 4.07525. We can also see that the rise in TIT causes an increase in ESFC.

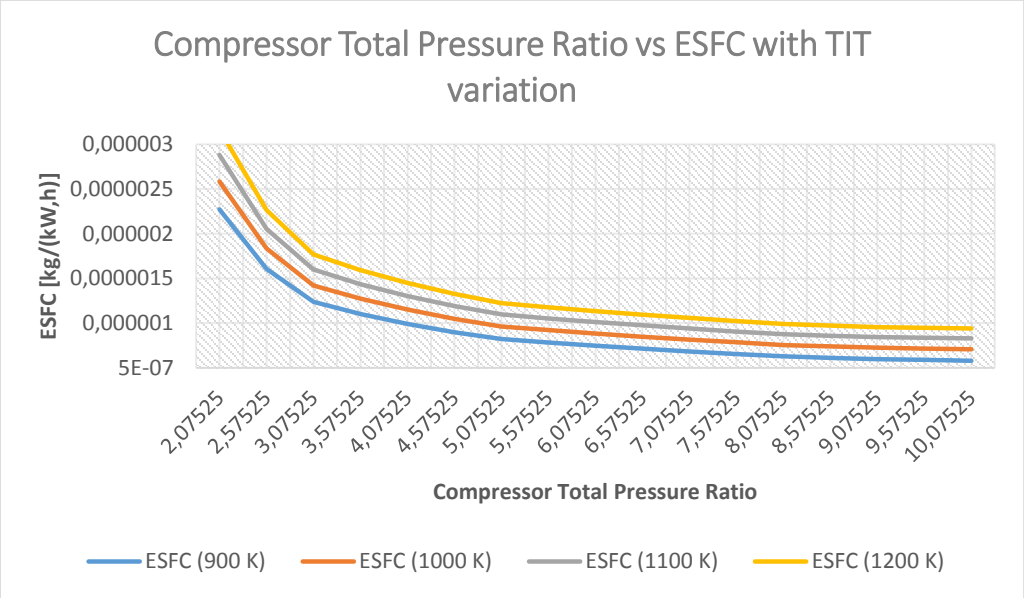

Figure 4.14 - Effect of Compressor Total Pressure Ratio on ESFC with a Turbine Inlet Temperature Variation

Figure 4.15 shows the effect of CTPR on EPW for several TIT's. The EPW increases with increasing TIT and increasing CTPR up to a pressure ratio of 9.07525. From that point on CTPR, there is a decrease in EPW, being considered the optimal point. Thus, for a pressure ratio of 9,07525 specific consumption is 8,435*10^-7 kg/kW.h.

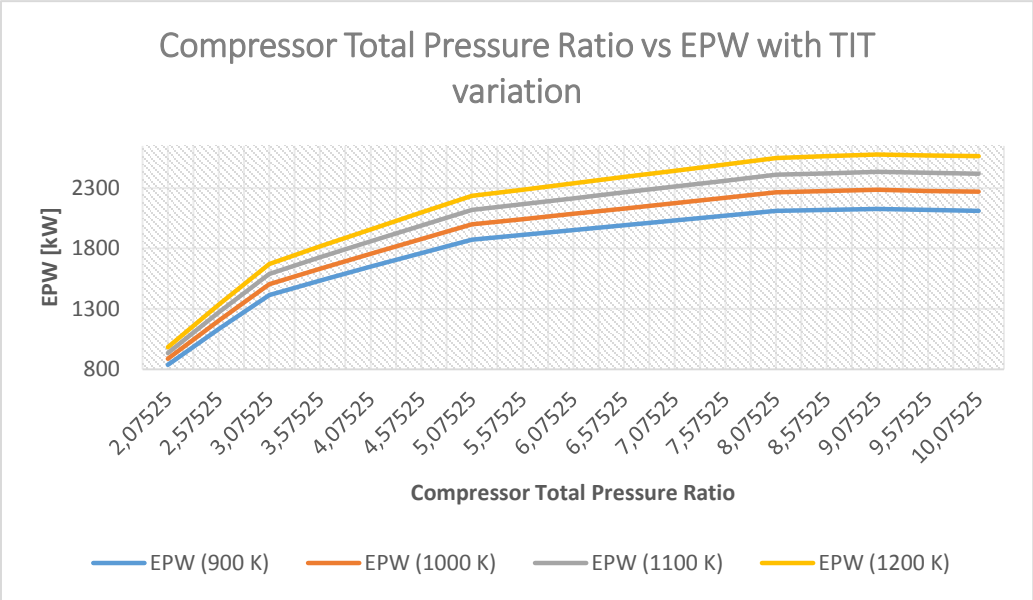

Figure 4.15 - Effect of Compressor Total Pressure Ratio on EPW with a Turbine Inlet Temperature Variation

Figure 4.16 demonstrates the effect of CTPR on TSFC for several TITs, the increase of which causes an increase in TSFC. For a 900 K TIT, thrust specific fuel consumption increases up to a pressure ratio of 3.07525, for a 1000 K TIT, TSFC increases up to a CTPR of 5.07525, and for an 1100 K TIT, TSFC increases up to a pressure ratio of 8.07525. From these pressure ratio values, TSFC decreases for each TIT value. For the 1200K TIT, the TSFC increases without reducing the pressure ratio range studied.

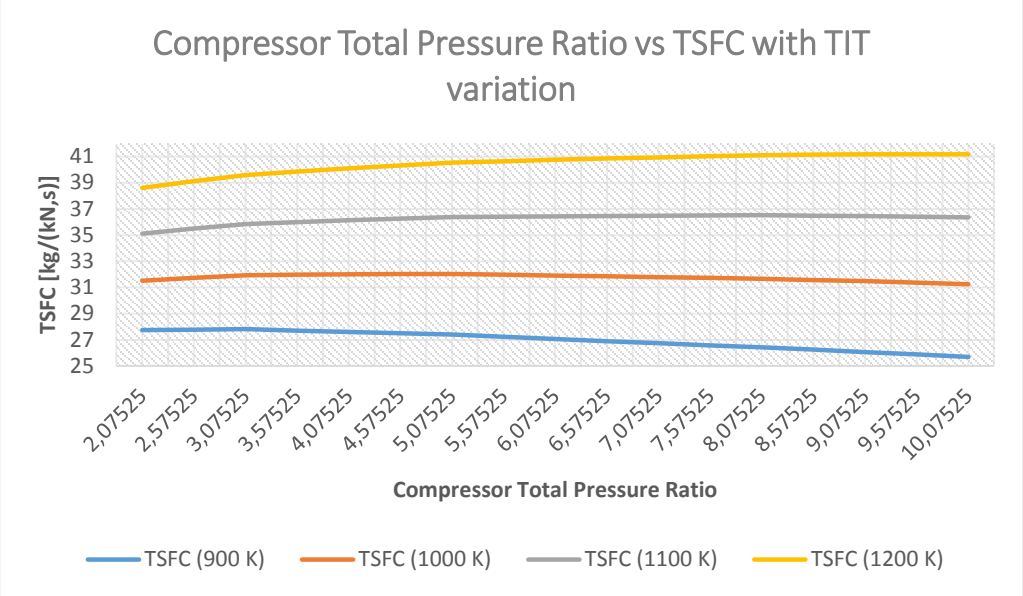

Figure 4.16 - Effect of Compressor Total Pressure Ratio on TSFC with a Turbine Inlet Temperature Variation

The increase in TIT causes an increase in Fnet (figure 4.17). However, we can also observe that with the rise of the pressure ratio in the compressor, the Fnet decreases considerably.

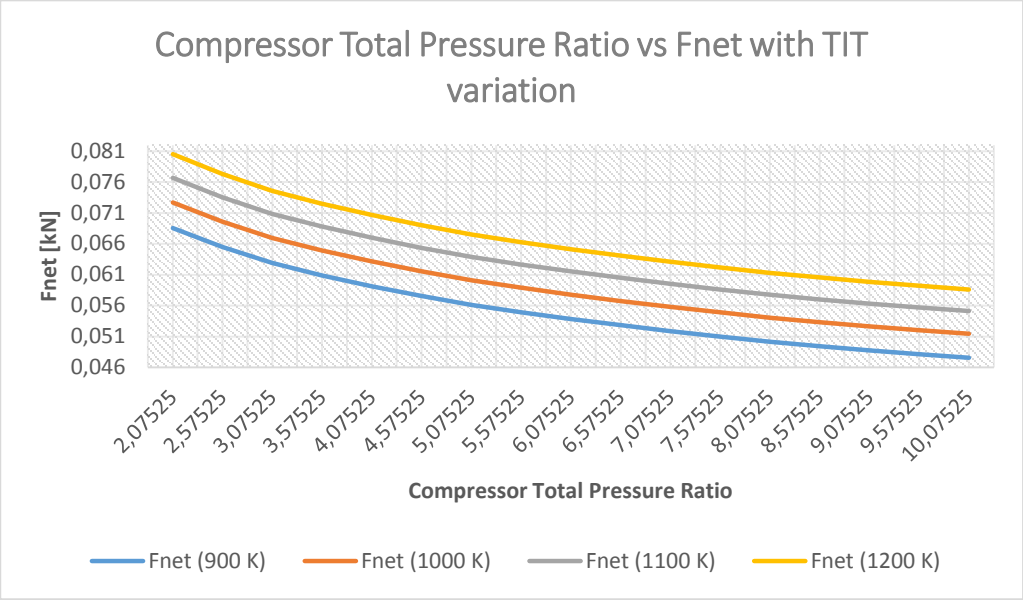

Figure 4.17 - Effect of Compressor Total Pressure Ratio on Fnet with a Turbine Inlet Temperature Variation

We can say, through the analysis of figure 4.18, that the PSFC has a more notable decrease for a pressure ratio between 2.07525 and 4.07525, and for higher values of CTPR the decline becomes a little less evident. We can also see that the increase in TIT causes a small rise in PSFC.

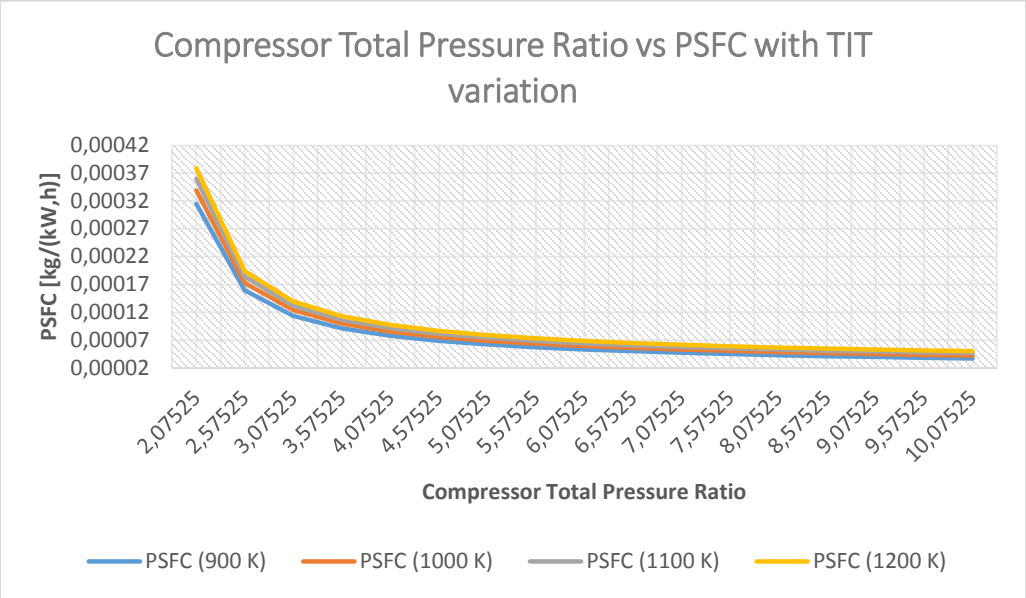

Figure 4.18 - Effect of Compressor Total Pressure Ratio on PSFC with a Turbine Inlet Temperature Variation

4.4 Turbine Inlet Temperature Effect

Figure 4.19 shows the behavior of the ESFC with the variation of the turbine inlet temperature for various flight speeds. The first conclusion we can draw from this analysis is the fact that for higher flight speeds consumption decreases. When analyzing the behavior of the ESFC with the variation of the TIT, we can see that there is a more noticeable decrease for a lower temperature reaching a minimum for the various flight speeds and, subsequently, the increase is very slight.

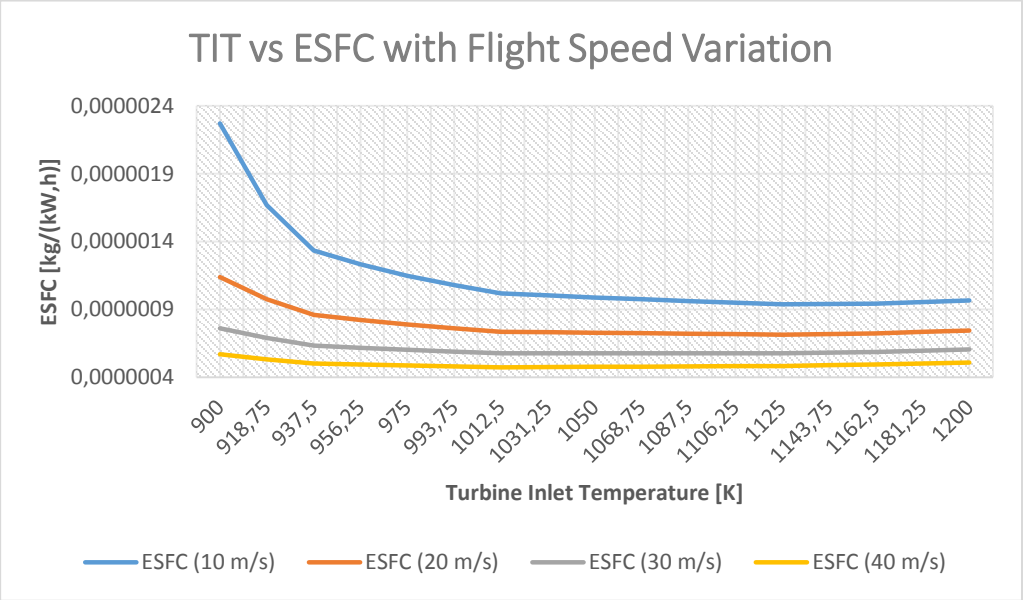

Figure 4.19 - Effect of TIT on ESFC with Flight Speed Variation

Concerning to EPW (figure 4.20), we can see that it increases with the increase of TIT and that the flight speed has a significant impact on this parameter, increasing EPW considerably for higher flight speeds.

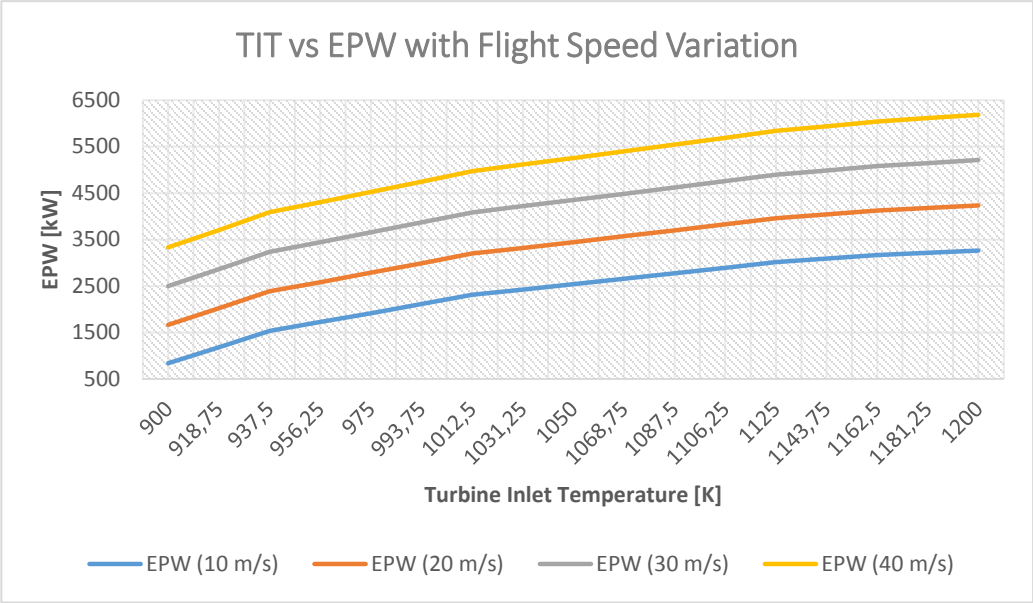

Figure 4.20 - Effect of TIT on EPW with Flight Speed Variation

Through Figure 4.21, we can see that the growth of TSFC is linear as a function of TIT. It is also worth noting that the increase in flight speed influences consumption since, for higher flight speeds, the TSFC is higher.

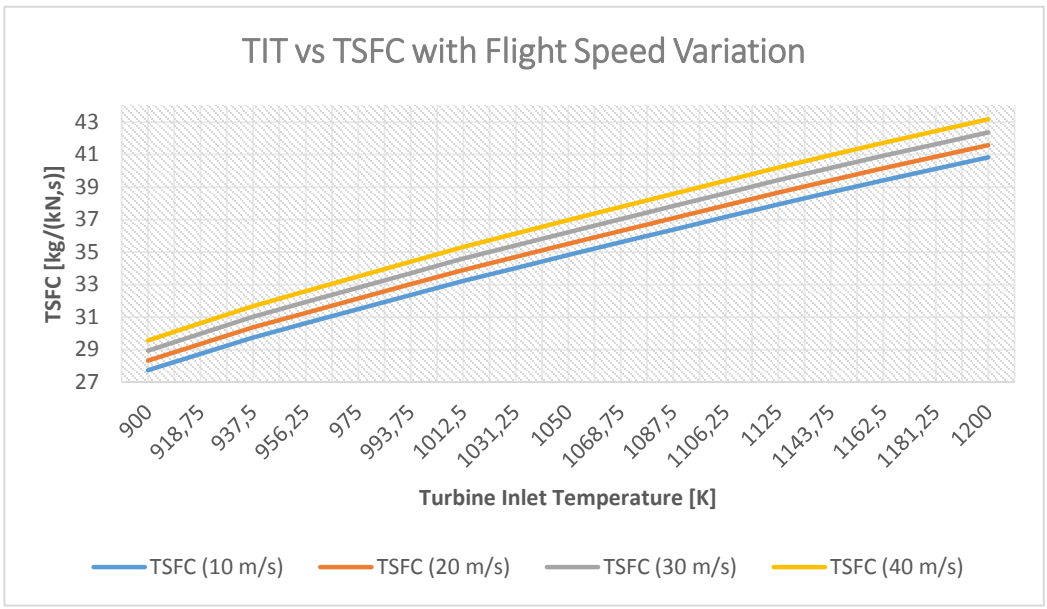

Figure 4.21 - Effect of TIT on TSFC with Flight Speed Variation

The increase in TIT causes an almost linear increase in Fnet and this increase becomes more evident for a temperature above 937.5 K (Figure 4.22). We can also see that, for higher speeds, Fnet decreases.

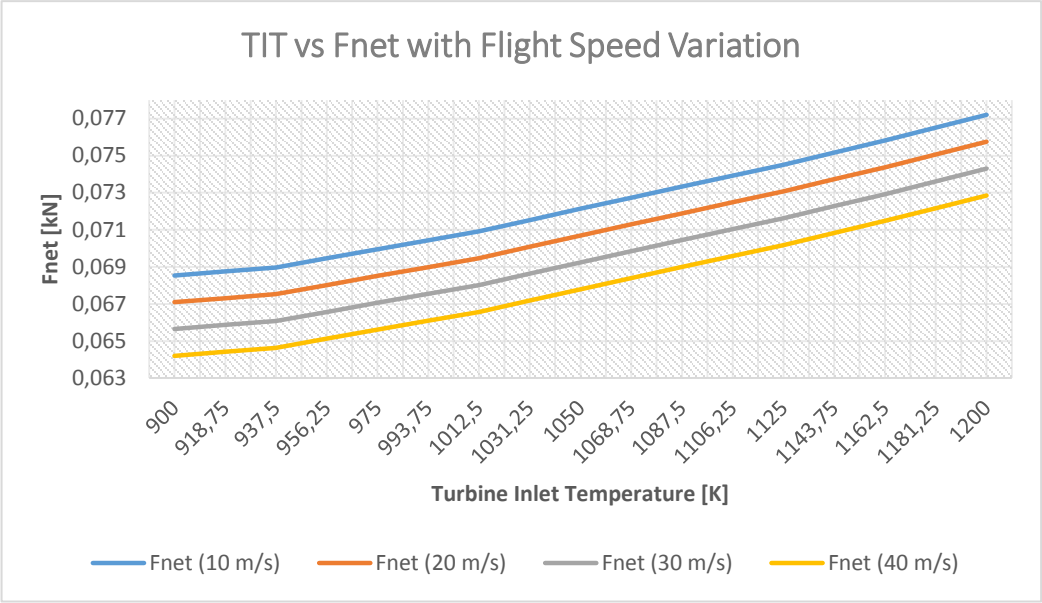

Figure 4.22 - Effect of TIT on Fnet with Flight Speed Variation

Figure 4.23 shows the behavior of the PSFC as a function of the turbine inlet temperature for various flight speeds. Thus, we can see that the increase in TIT causes a linear growth in PSFC, and the flight speed does not have a significant impact on this parameter.

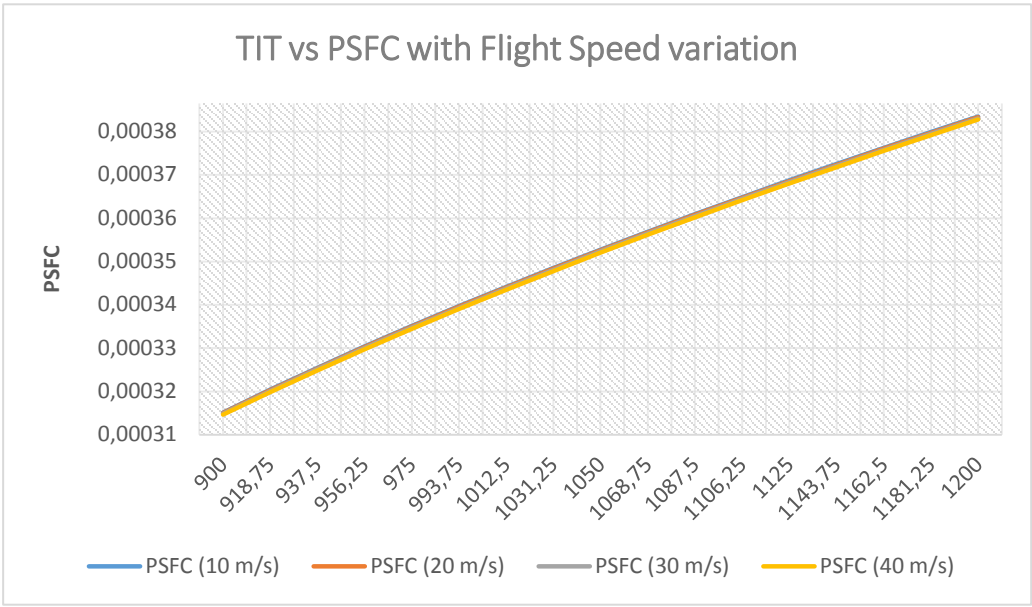

Figure 4.23 - Effect of TIT on PSFC with Flight Speed Variation

4.5 Flight Speed Effect

Regarding the EPW, we can see (Fig. 4.24) that for higher speeds, the shaft power also increases and, for speeds more elevated than the one studied, its increase becomes less significant.

Concerning the ESFC (Fig. 4.24), we can see that there is a considerable decrease in consumption that will become less and less noticeable as the speed increases.

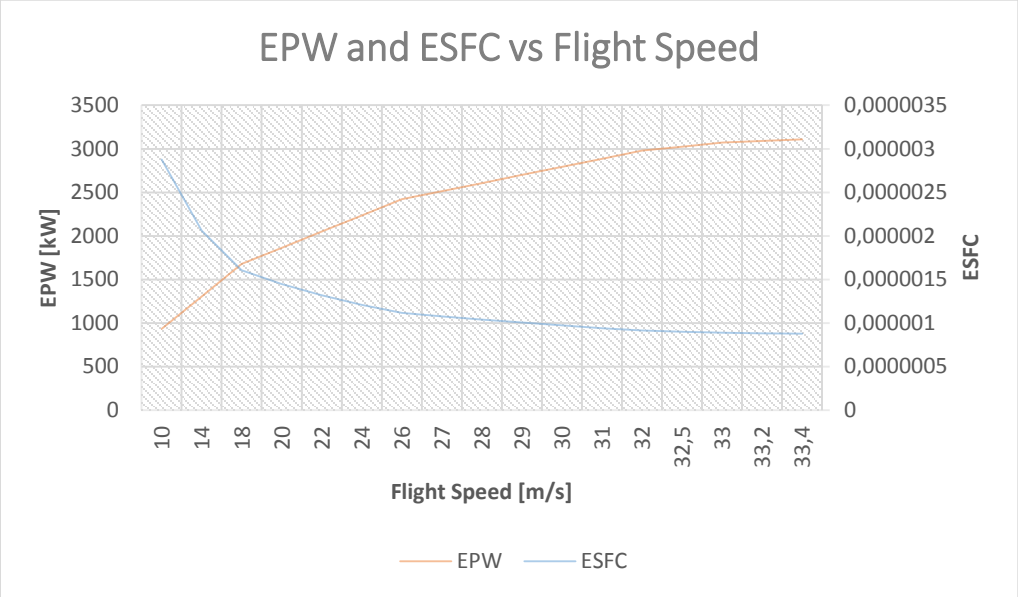

Figure 4.24 - Effect of Flight Speed on EPW and ESFC

Concerning Fnet, we can observe (Fig. 4.25) that for higher speeds, the thrust decreases considerably in the deliberate speed and that for higher values, its decrease would be less accentuated. TSFC, being related to Fnet, has a marked increase for this speed range making it less evident after 33 m/s.

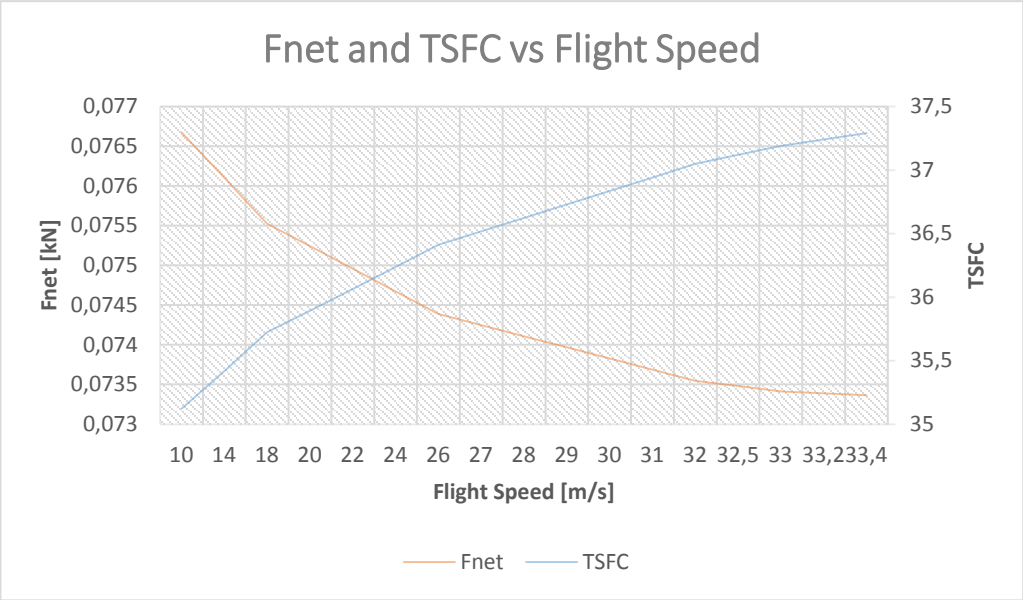

Figure 4.25 - Effect of Flight Speed on Fnet and TSFC

Figure 4.26 shows the behavior of the PSFC as the flight speed increases. Thus, we can observe that there is an exponential growth of the PSFC with the increase in speed.

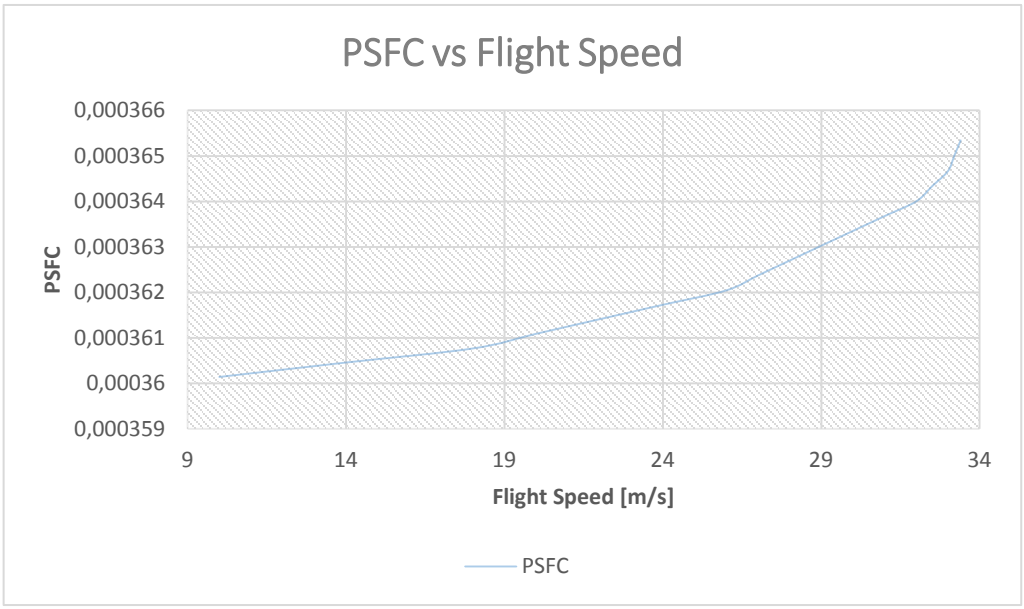

Figure 4.26 - Effect of Flight Speed on PSFC

Chapter 5

5. Conclusion and Possible Future Works

5.1 Conclusion

The aeronautical industry is an industry in constant evolution. In recent years, the search for the adaptation of drones to surveillance and reconnaissance activities, of cargo transportation has been increasing. However, most drones have an electric propulsion or combustion system. Concerning the use of gas turbines, there is more excellent knowledge and research on small turbojet engines. Since the turboprop engine is an efficient engine for short to medium range and lower altitudes it has a good load and specific consumption ratio it would be interesting to know the feasibility of using this type of engines with small dimensions.

Thus, this study had the main objective of creating a design point for a turboprop micro motor through performance equations used for the study of the Honeywell TPE331 engine (used by the General Atomics MQ-9 Reaper better known as Predator B) and making the parametric study.

The parameters used were altitude, the airflow at intake, compressor total pressure ratio, the turbine inlet temperature and the flight speed which, through the variation of each one, the objective was to understand the behavior of equivalent specific fuel consumption (ESFC), thrust specific fuel consumption (TSFC), power specific fuel consumption (PSFC), equivalent shaft power (EPW) and total net thrust (Fnet).

The study was carried out under the International Standard Atmosphere (ISA) conditions, and the independent parameters were varied as follows:

- The altitude was varied between 0 m and 1600 m.
- The airflow at the intake took the values of 0.1145 kg/s, 0.1445 kg/s, 0.1745 kg/s and 0.2045 kg/s.
- The compressor total pressure ratio was varied between 2.07525 and 10.07525.
- The turbine inlet temperature was varied between 900 K and 1200 K.
- The flight speed was varied between 10 m/s and 33.4 m/s.

Regarding the altitude variation for various ratios of total pressure in the compressor, we can see that there was no significant change in the ESFC, EPW and TSFC. However, it is concluded that the increase in the pressure ratio decreases Fnet and PSFC considerably.

Concerning the airflow at the intake, we can conclude that it does not affect specific consumption. However, for higher airflow, both shaft work and total thrust increase considerably. A variation of 0.09 kg/s in the airflow causes an increase to, approximately, double the thrust.

Regarding CTPR, we can see that its influence on PSFC is minimal. However, we can see that, for all TITs, there is a reduction of about 70% in ESFC. Regarding the EPW, we can see that it reaches a maximum that will be the optimum point of equivalent shaft power. It is also worth noting that the variation in CTPR does not cause a significant change in the TSFC, and for a higher TIT, the TSFC increases considerably. With Fnet we can see that the increase in CTPR causes a reduction of about 31% with similar behavior for the various TITs, higher the TIT, higher the Fnet.

The variation of the inlet temperature in the turbine is an essential factor in the performance of the engine. We can see that it causes a considerable increase in EPW and Fnet and for higher speeds EPW increases, which is the opposite of what happens for Fnet. For PSFC, the variation in TIT causes an increase of about 18%, but the difference in speeds causes a minor change.

Regarding the flight speed, it should be noted that, for higher flight speeds, the PSFC grows exponentially. As ESFC depends on EPW, one would expect the opposite behavior of the other parameter where there is an increase in EPW and a decrease in ESFC. Regarding Fnet and TSFC, the opposite of the previous parameters would be expected, leading to the conclusion that, for higher flight speeds, Fnet decreases and TSFC increases.

5.2 Possible Future Works

In this work, the design point and parametric study of a micro two-spool turboprop were carried out. It would be interesting to compare the design point and the parametric study obtained using programs like GasTurb or Simulink.

It would also be interesting to proceed to its detailed project and, later, to its construction, being able to make a comparative study on the theoretical analysis and the practical results.

References

Center for Naval Aviation Technical Training. (1991). *Aviation Machinist's Mate 3 & 2 (NAVEDTRA 14008)*. http://navybmr.com/study material/14008a/14008A_ch8.pdf

Chaput, A. J. (2010). Rapid air system concept exploration - A parametric physics based system engineering design model. *10th AIAA Aviation Technology, Integration and Operations Conference 2010, ATIO 2010*, *3*(September).

Dinç, A. (2015). Sizing of a turboprop unmanned air vehicle and its propulsion system. *Isi Bilimi Ve Teknigi Dergisi/ Journal of Thermal Science and Technology*, *35*(2), 53–62.

El-Sayed, A. F. (2016). Fundamentals of aircraft and rocket propulsion. In *Fundamentals of Aircraft and Rocket Propulsion*. https://doi.org/10.1007/978-1-4471-6796-9

El-Sayed, A. F. (2017). *Aircraft Propulsion and Gas Turbine Engines (Second Edition)* (Taylor & Francis (ed.)). CRC Press.

F. El-Sayed, A. (2016). Aero-Engines Intake: A Review and Case Study. *Journal of Robotics and Mechanical Engineering Research*, *1*(3), 35–42. https://doi.org/10.24218/jrmer.2016.15

FAA. (2016). Transition to Turbopropeller-Powered Airplanes. *Airplane Flying Handbook FAA (Federal Aviation Administration)-H-8083-3B*, *Chapter 14*, 1–14.

Kurzke, J. (2007). *GasTurb 11 User Manual, Design and Off-Design Performance of Gas Turbines*.

Kyprianidis, K. G., Gkoudesnes, C., & Camilleri, W. (2015). Gas Turbines for Power and Propulsion. *Handbook of Clean Energy Systems*, *2*, 1–25. https://doi.org/10.1002/9781118991978.hces140

Large, J., & Pesyridis, A. (2019). Investigation of micro gas turbine systems for high speed long loiter tactical unmanned air systems. *Aerospace*, *6*(5), 1–36. https://doi.org/10.3390/AEROSPACE6050055

Mattingly, J. (1996). Elements of Gas Turbine Propulsion. In *Tata McGraw-Hill* (Vol. 2005).

Rolls-Royce. (1996). *The Jet Engine*. Rolls-Royce plc.

Saravanamuttoo, H., Rogers, G., & Cohen, H. (2006). *Gas Turbine Theory* (Pearson (ed.); 5th Editio).

Sinha, C. K., & Narayan, P. D. (2015). *Brayton Cycle & Variations*.

Skybrary. (2019). *AP4ATCO - Turboprop Engine*. https://www.skybrary.aero/index.php/AP4ATCO_-_Turboprop_Engine

Teeuwen, Y. A. P. (2017). Propeller Design for Conceptual Turboprop Aircraft. *MSc Thesis, TU Delft*, 1–103. http://repository.tudelft.nl/.%0Ahttps://repository.tudelft.nl/islandora/object/uuid:d746a647-25e1-463b-af3a-6c2c478e1b37/datastream/OBJ/download

Tsai, L. (2004). *Design and Performance of a Gas-Turbine Engine from an Automobile Turbocharger*. Massachusetts Institute of Technology.

Walsh, P. P., & Fletcher, P. (2004). Gas Turbine Performance, 2nd Edition. In *Blackwell*

Science.

Wikiwand. (2020). *Wikiwand*. https://www.wikiwand.com/en/Propelling_nozzle